e⁻CLOUD'18

SEY and other material properties studies at cryogenic temperatures

L. Spallino[1], M. Angelucci[1], R. Larciprete[1, 2]
and R. Cimino[1]

[1] LNF-INFN, Frascati, Italy
[2] CNR-ISC, Roma, Italy

FCC hh ee he

INFN
Istituto Nazionale di Fisica Nucleare

EuroCirCol
A key to New Physics

Outline

- Introduction
  - Surface sensitivity of SEY
  - SEY at cryogenic temperature
  - Vacuum stability at cryogenic temperature
- Strategy and experimental set-up at LNF
- Results
  - Adsorption/desorption kinetics by SEY and TPD
  - TPD of Ar on LASE-Cu for vacuum stability studies

Surface sensitivity of SEY

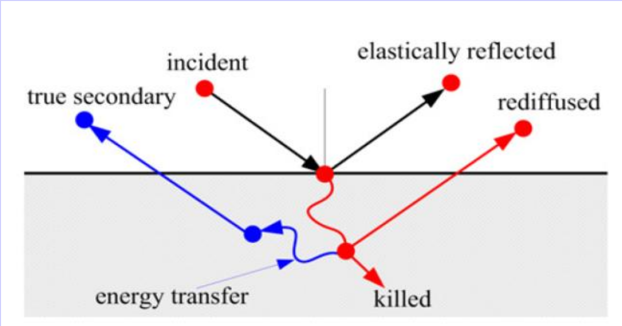

Secondary Electron Emission

Three-step process:

- Production of SE at a depth *z*
- Transport of the SE toward the surface
- Emission of SE across the surface barrier

Electron mean free path up to ~10 nm (few monolayers)

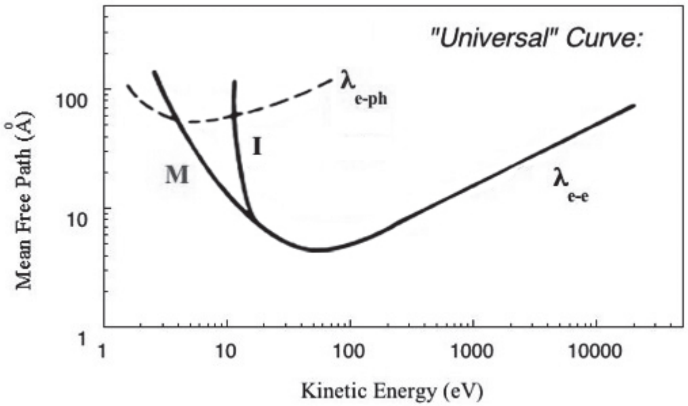

Surface conditions influence SEY measurements

R. Cimino & T. Demma, Int. J. Mod. Phys. A (2014)

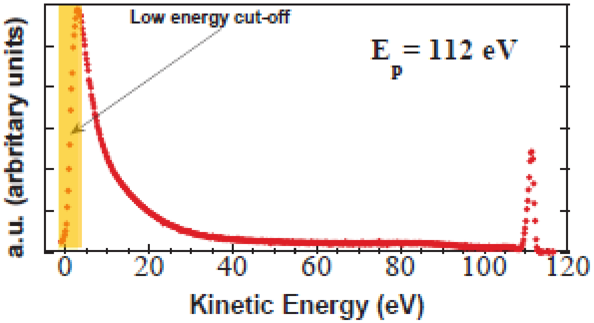

Energy Distribution Curve (EDC) of the electrons produced by a 112 eV primary energy electron beam impinging on a Cu technical surface

SEY and chemical state of the surface

From the talk "SEY from noble metals" given by L. GONZALEZ GOMEZ

Effect of contaminants of the atmosphere

SEY measurements at room temperature

L. A. Gonzalez et al., AIP Adv. (2017)

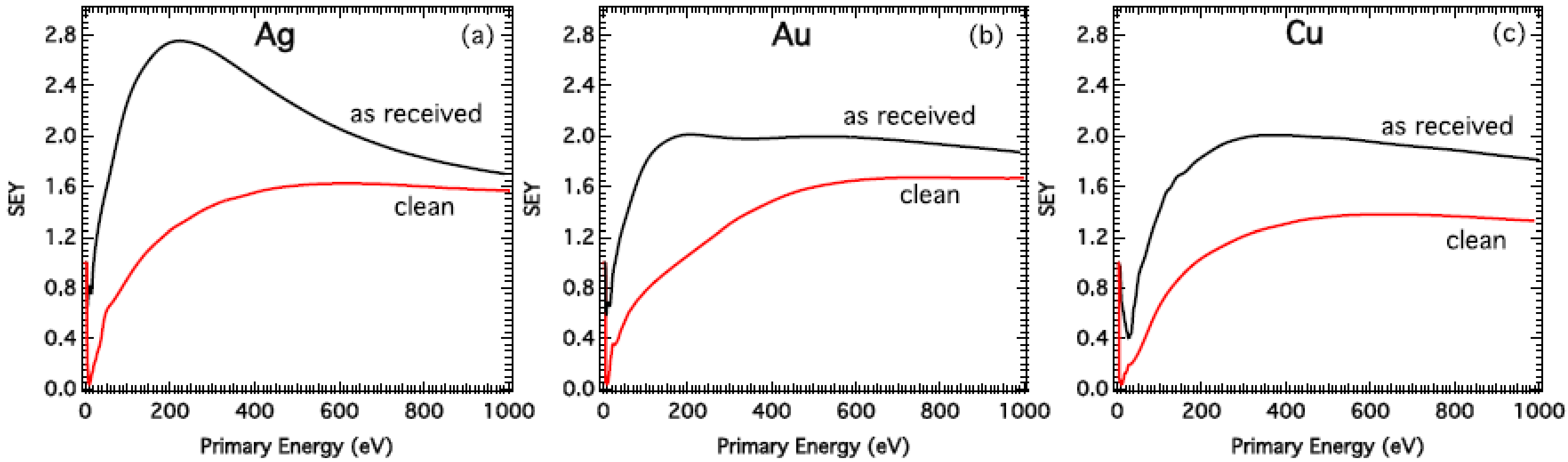

<u>Chemisorbed</u> compounds modify the chemical bonds at the metal surface and interact directly with the impinging electrons

SEY at cryogenic temperature

Kuzucan et al., J. Vac. Sci. Technol. A (2012)

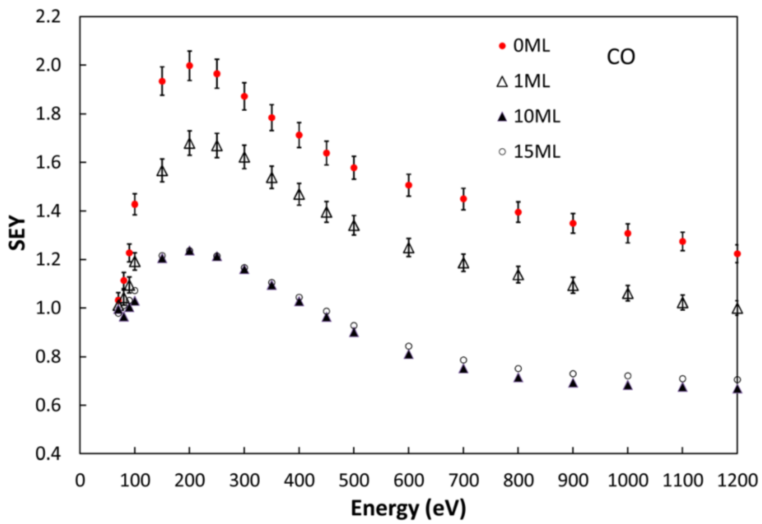

SEY as measured on a Cu surface held at 4.7 K as a function of increasing CO coverage

SEY of cold surfaces influenced by gas <u>physisorption</u>

Residual gas in a vacuum

L. A. Gonzalez et al., AIP Adv. (2017)

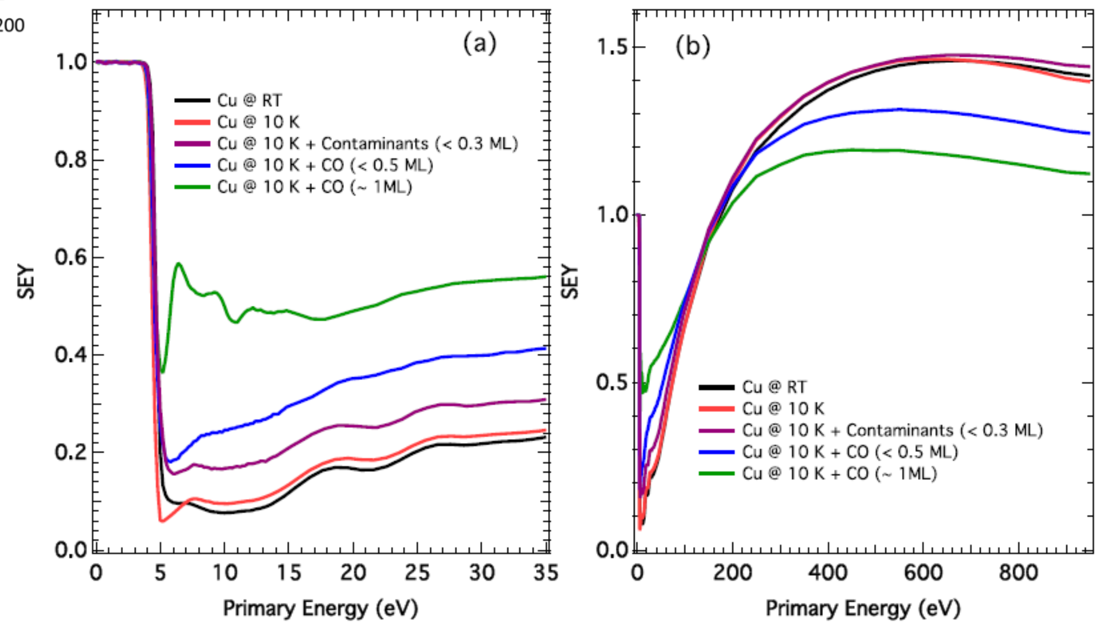

SEY is <u>highly sensitive</u> to the presence of adsorbates, <u>even at sub-monolayer coverage</u>

Study of SEY at cryogenic temperature for particles accelerators

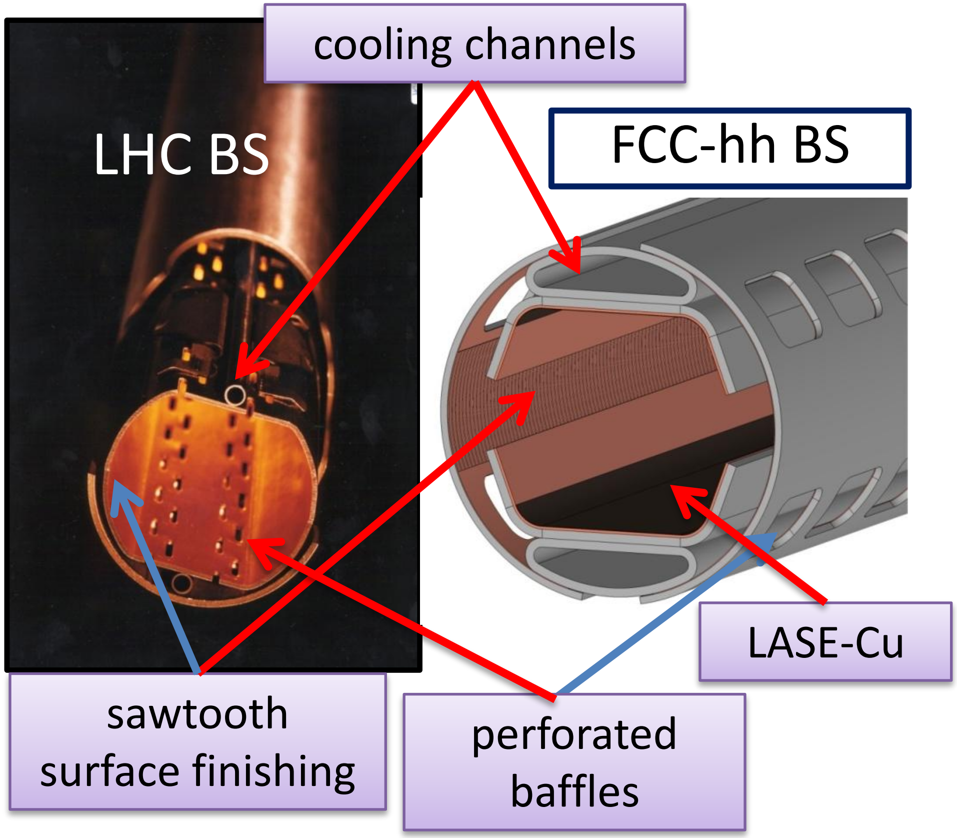

- **Low temperature (LHC beam screen T~5-20 K)**
- **UHV (P <10^{-11} mbar)**
- **Surface characteristics**

Study of SEY at cryogenic temperature for particles accelerators

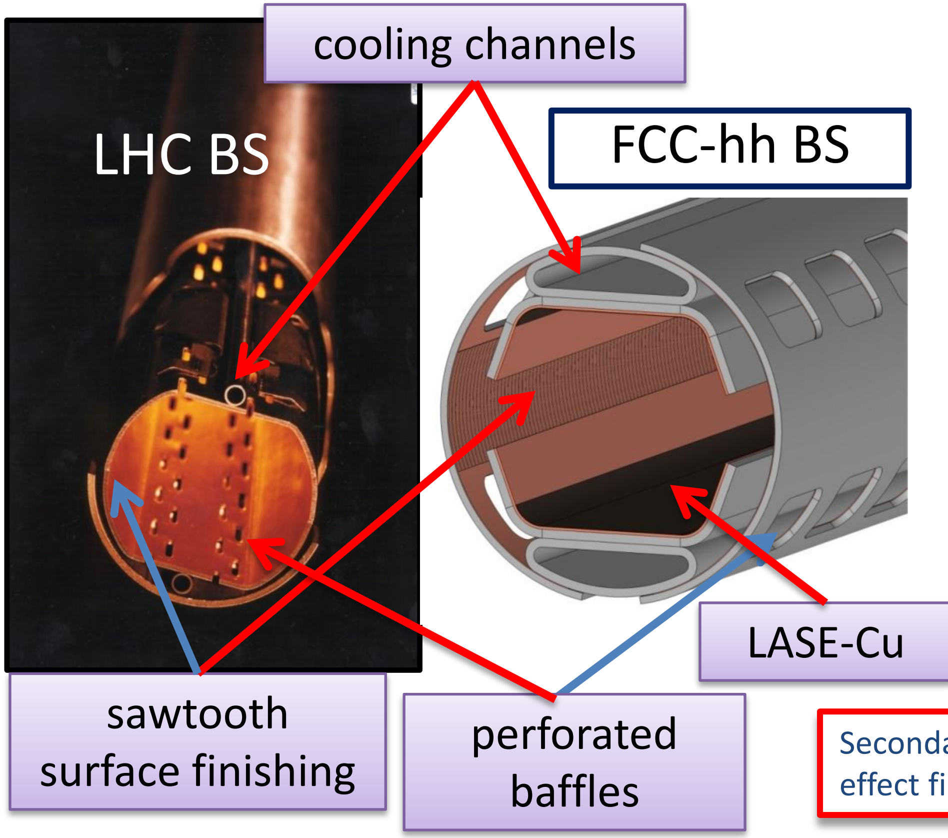

- **Low temperature (LHC beam screen T~5-20 K)**
- **UHV (P <10^{-11} mbar)**
- **Surface characteristics**

e^- cloud phenomenon

Secondary Electron Emission can drive an **avalanche multiplication** effect filling the beam chamber with an **electron cloud**

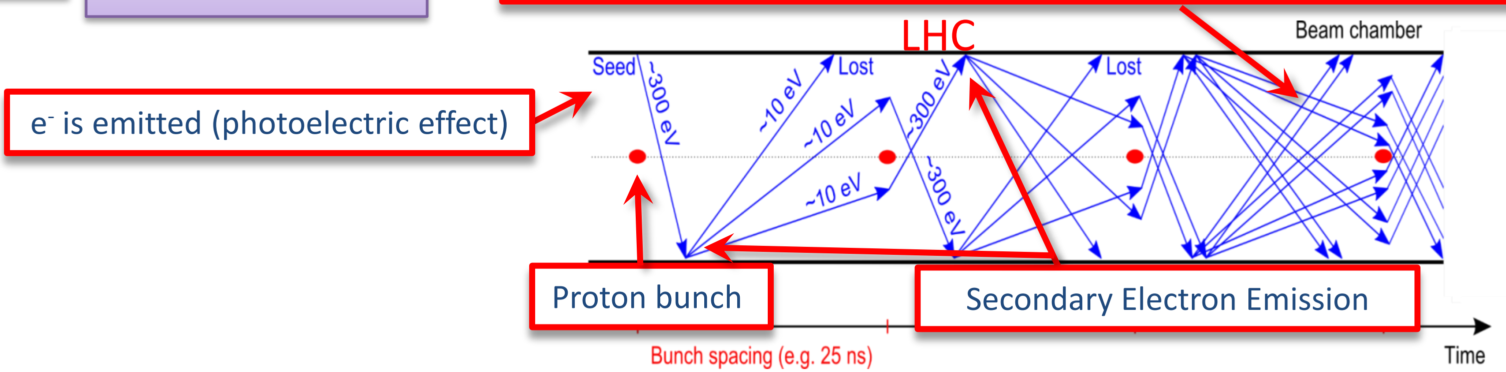

Mitigation of the beam induced effects by acting on the surface characteristics

R. Larciprete et al., Appl. Surf. Sci. (2015)

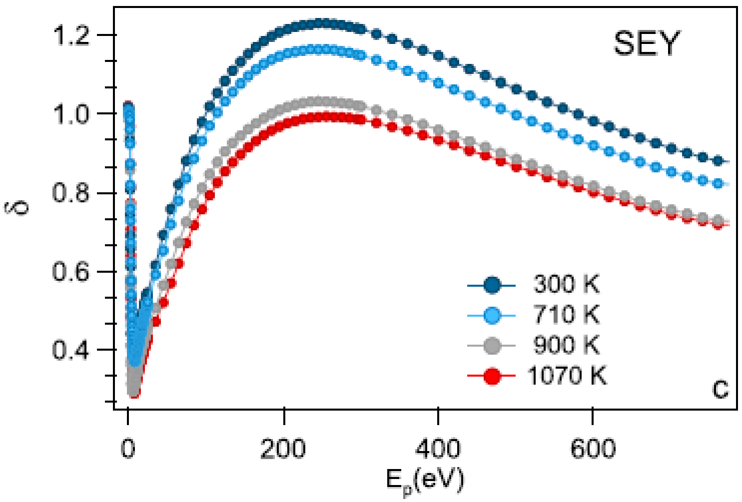

Modification of surface chemistry

Amorphous C-coating

(thermal graphitization of thin amorphous C layers deposited by magnetron sputtering on Cu substrates)

R. Valizadeh et al. , Appl. Phys. Lett. (2014)

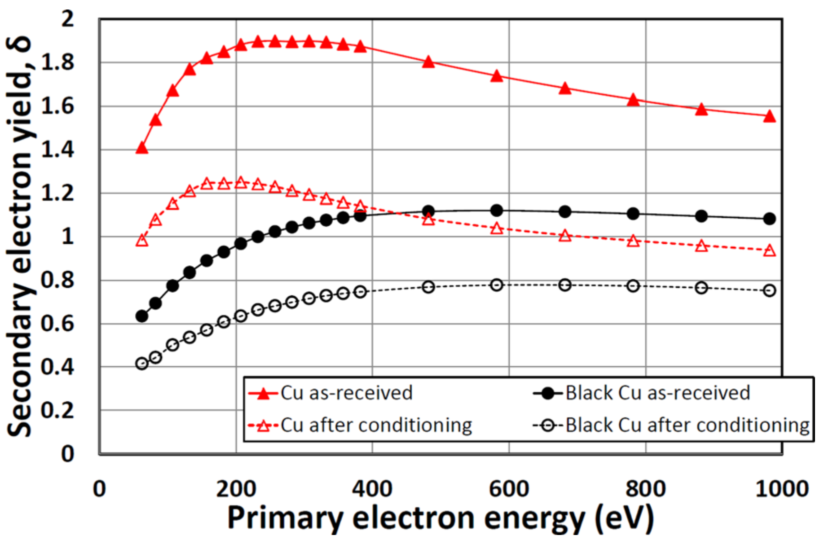

Engineering the surface morphology

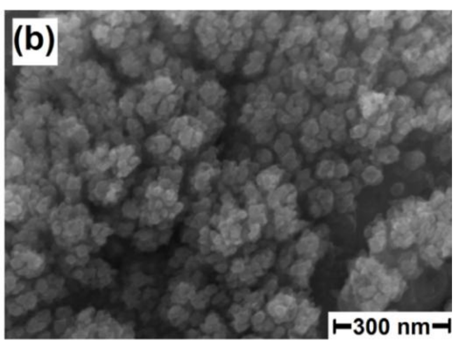

Laser ablation and conditioning

R. Valizadeh et al. , Appl. Surf. Sci. (2017)

Vacuum stability at cryogenic temperature

LHC
Synchrotron Radiation
Power = 0.13 W/m

FCC
Synchrotron Radiation
Power = 40 W/m

Temperature/Pressure Variation

↓

Beam life Time

Working Pressure ($<10^{-11}$ mbar) ⟷ **Beam screen Temperature Range**

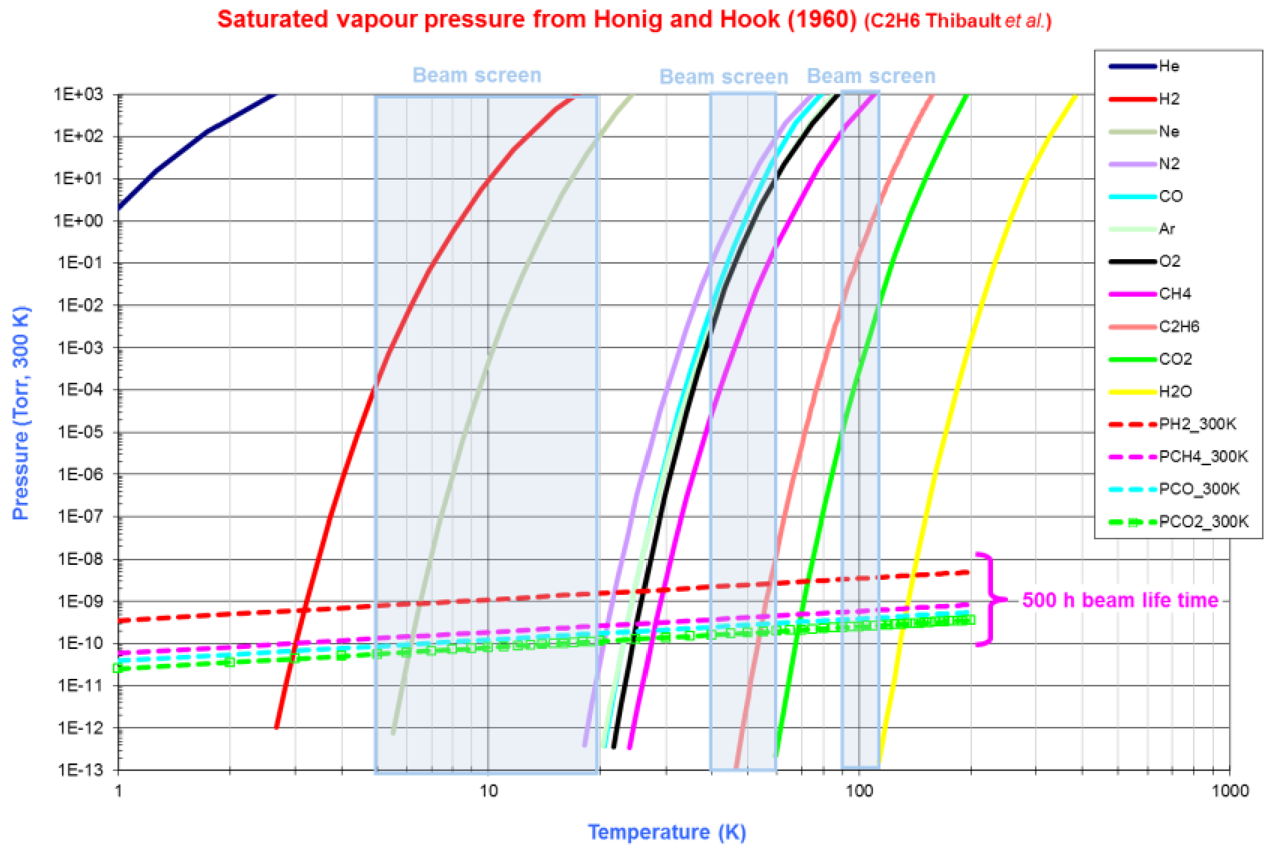

<u>Independently on the substrate treatment</u>, **the vacuum stability due to the desorption of residual contaminant gases has to be guaranteed**

Strategy and experimental set-up at LNF

Low Temperature

↓

Gas **Adsorption**

↓

SEY variation

Strategy and experimental set-up at LNF

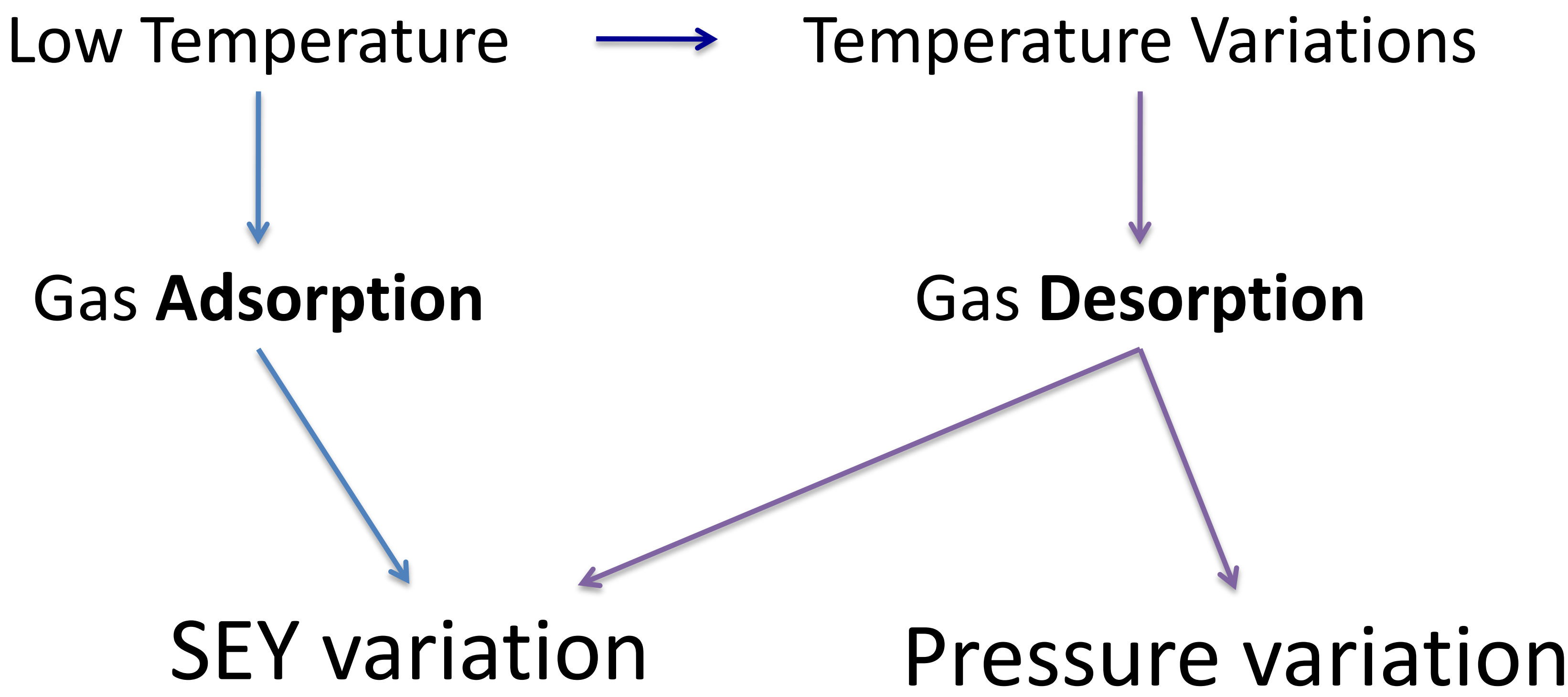

SEY and Thermal Programmed Desorption (TPD) as useful techniques to quantitatively follow adsorption/desorption kinetics

Strategy and experimental set-up at LNF

Ultra high vacuum systems

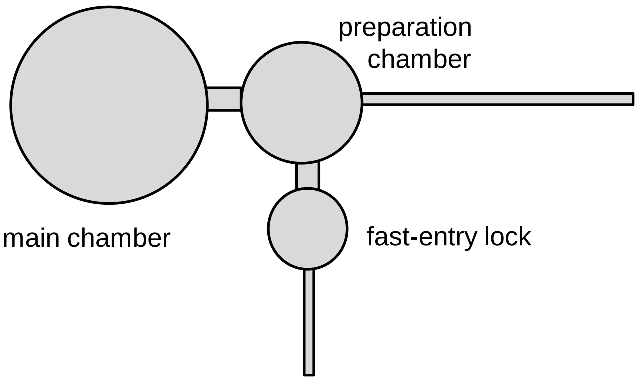

- LNF-cryogenic manipulator
- Sample at **15-300 K**

Secondary Electron Yield (SEY) measurements

Equipment : Electron gun, Faraday cup

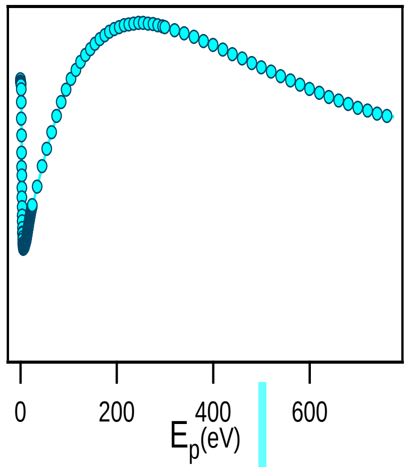

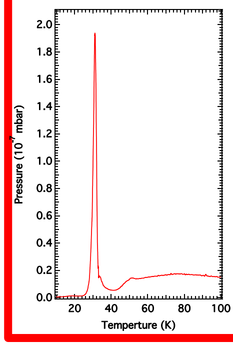

Temperature Programmed Desorption (TPD) measurements

Equipment : QMS (Hiden HAL 101 Pic)

Adsorption monitored by SEY

Proof of principle: Ar on clean Cu at T~15 K

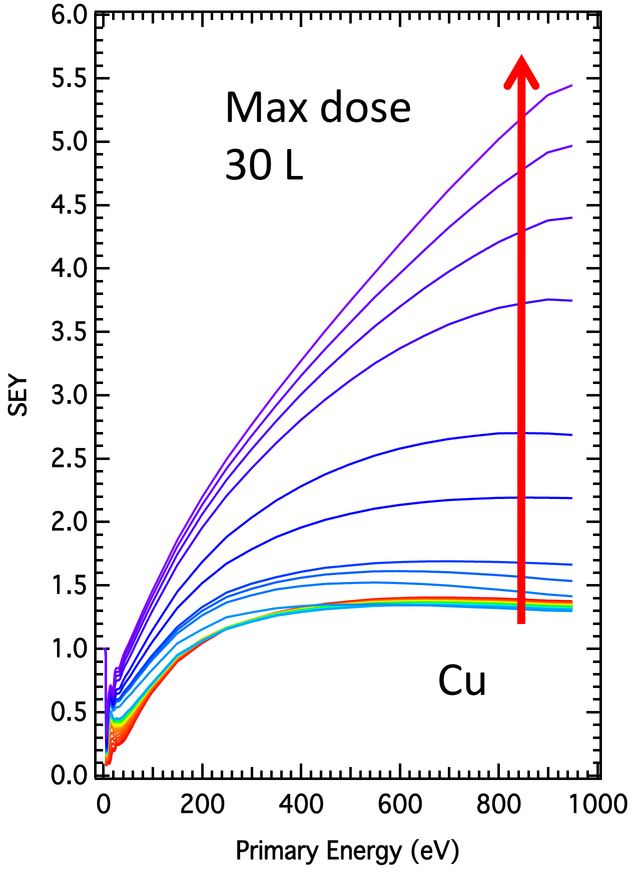

Adsorption monitored by SEY

Proof of principle: Ar on clean Cu at T~15 K

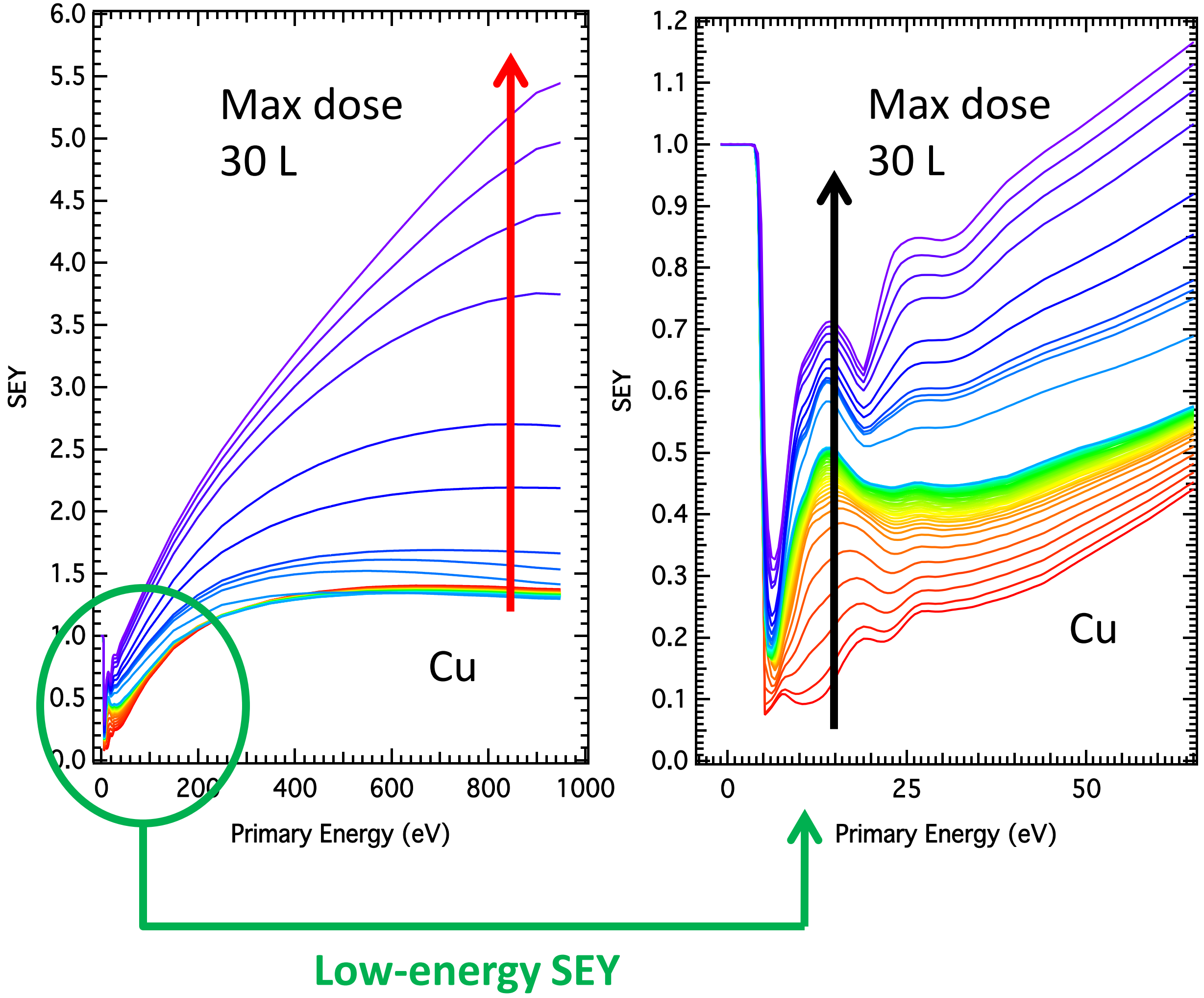

Adsorption monitored by SEY

Proof of principle: Ar on clean Cu at T~15 K

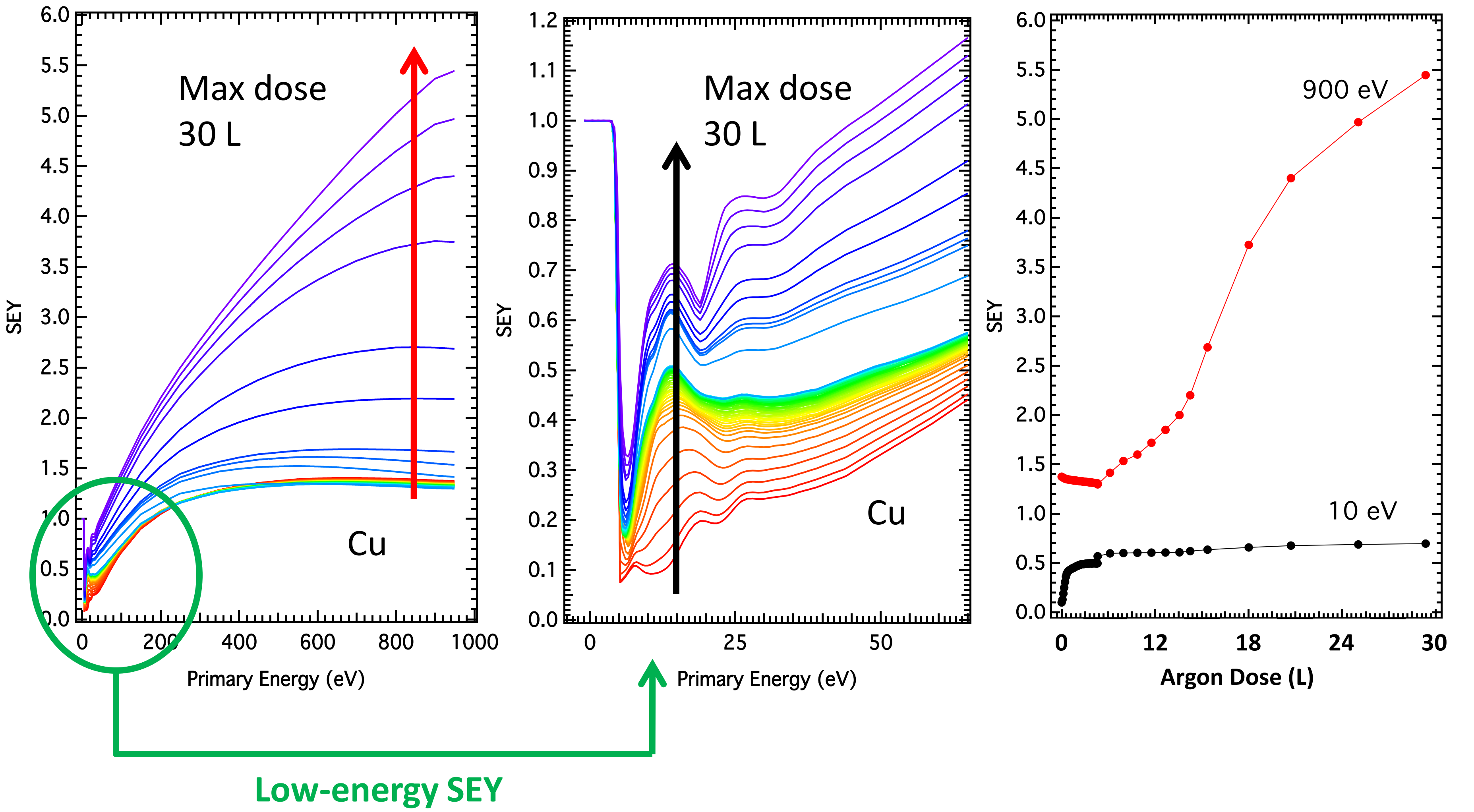

It's known that…

Energy Distribution Curves at different Primary Energy

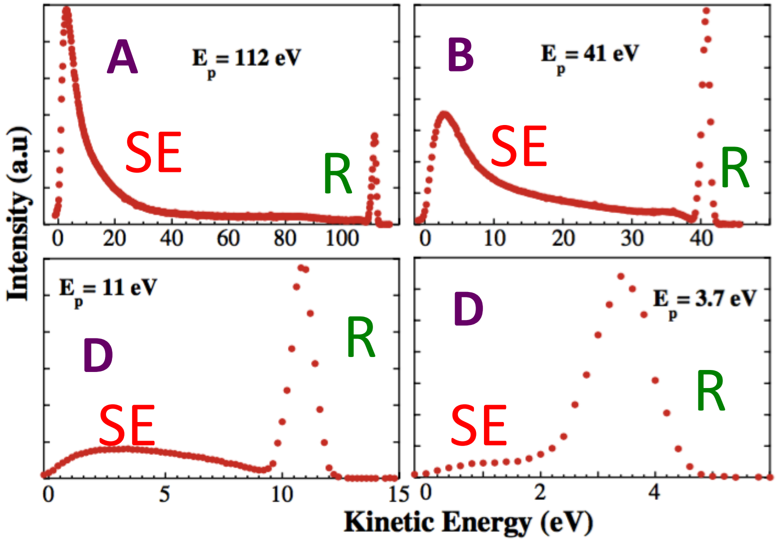

Cimino et al., PRL 93 (2004)

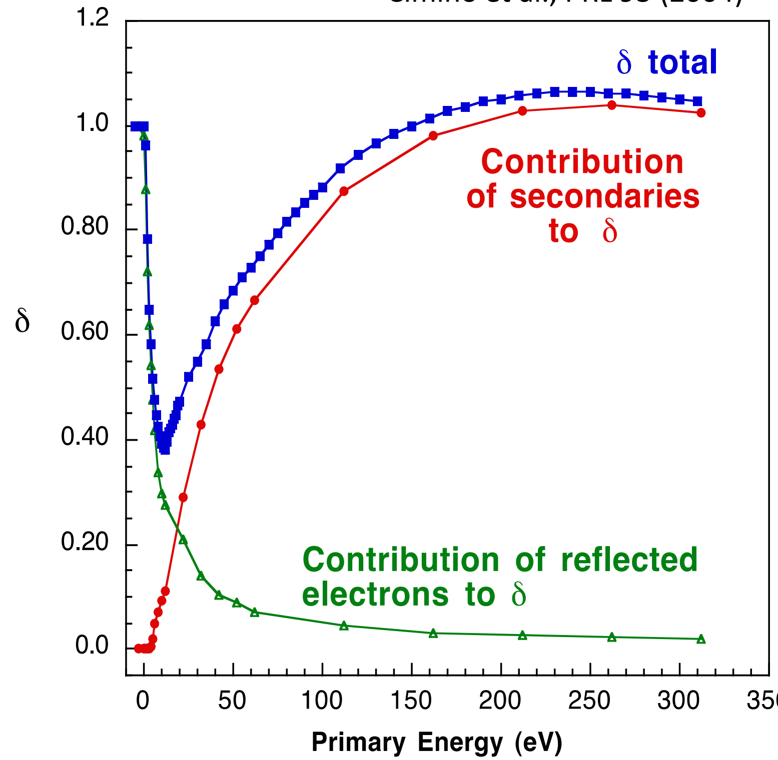

Low-Energy Range → Reflected electron component → Sensitive to surface variation

High-Energy Range → Total amount of emitted secondary electrons → Sensitive to thick layer

Adsorption monitored by SEY

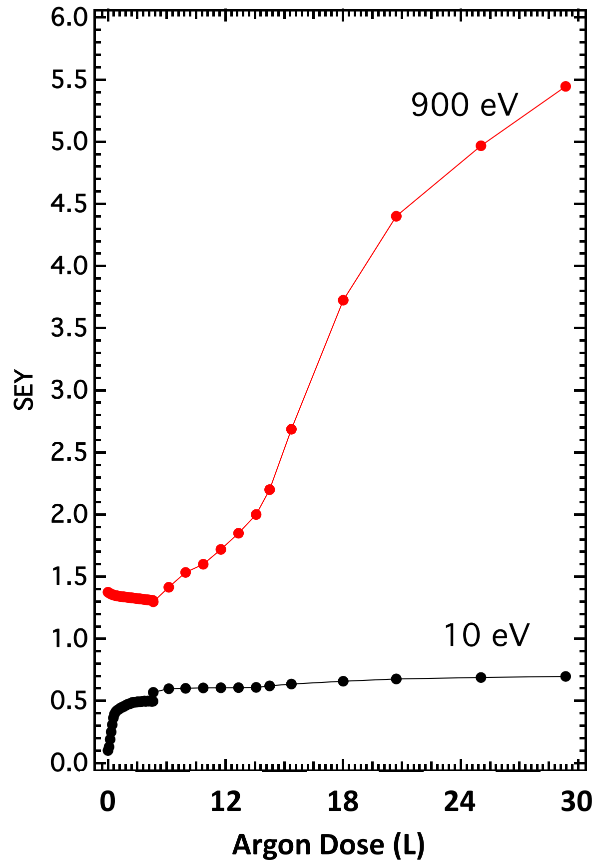

Adsorption monitored by SEY

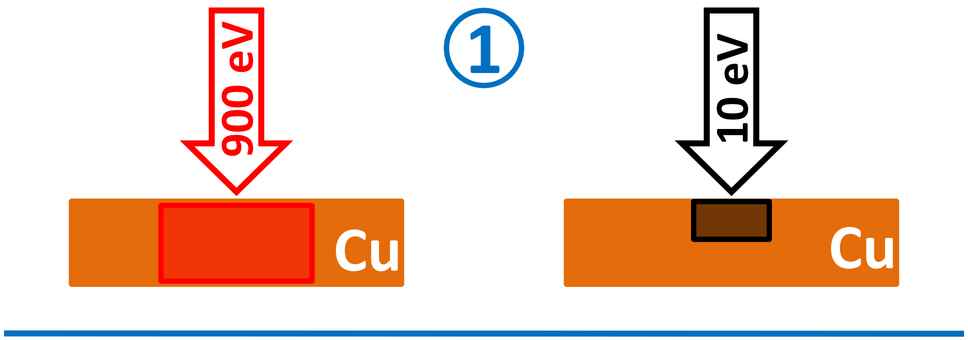

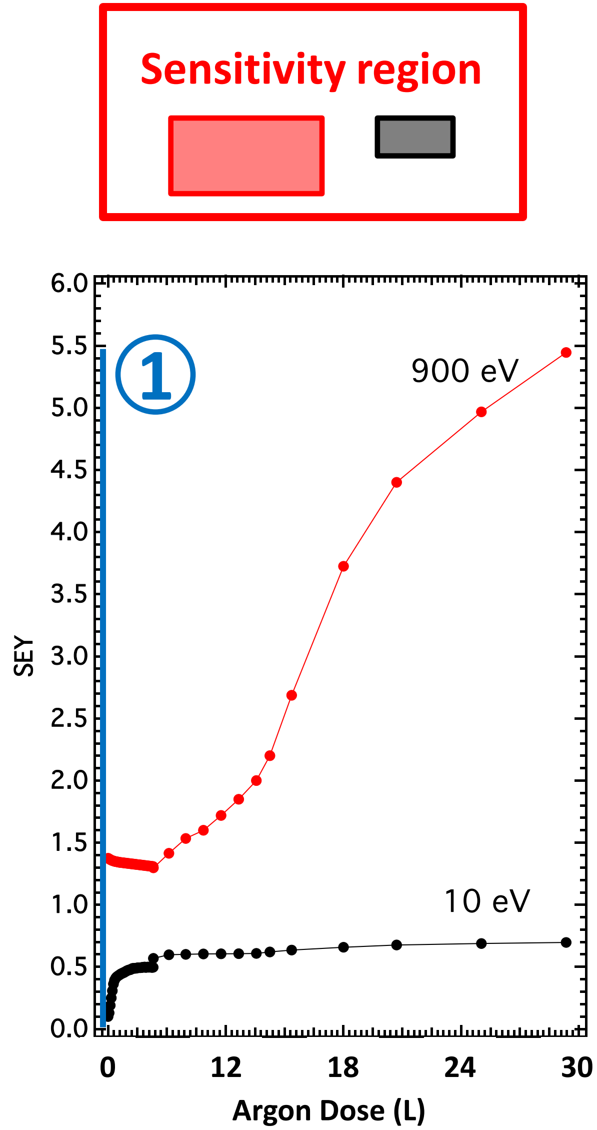

Adsorption monitored by SEY

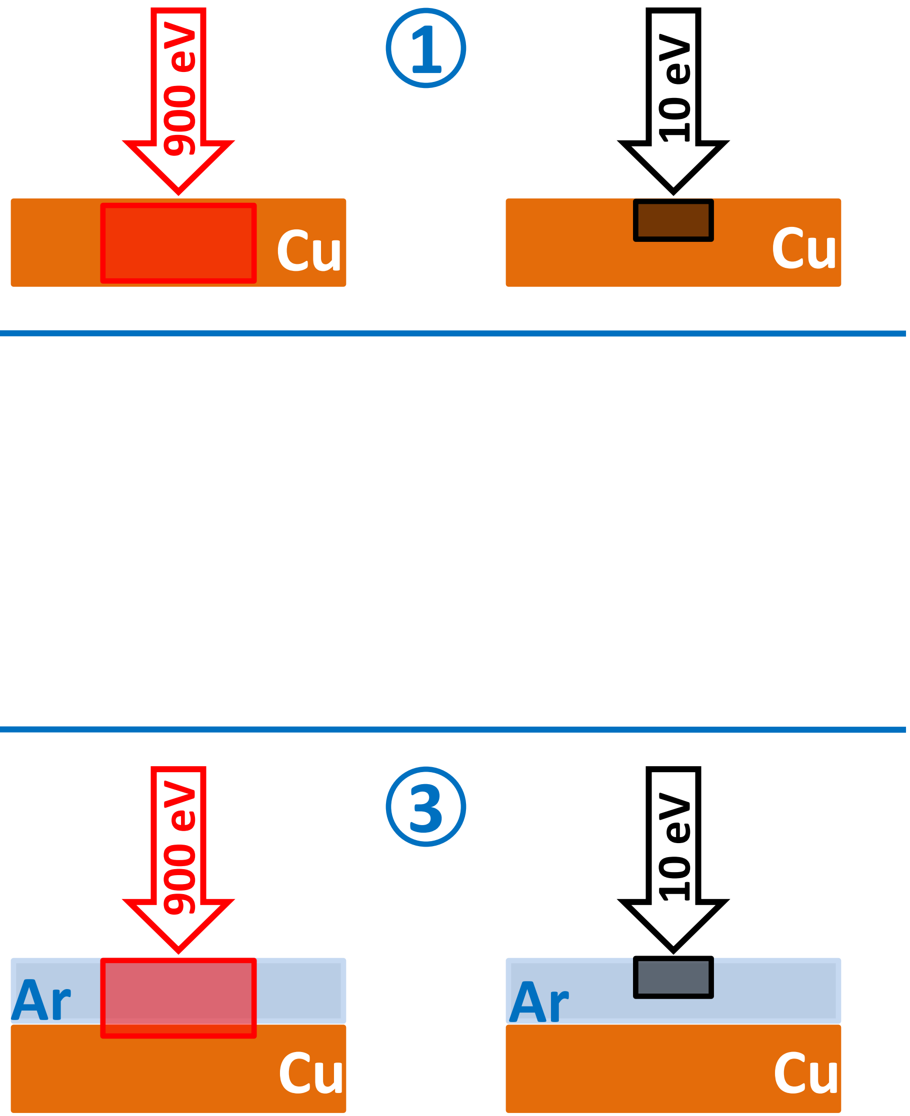

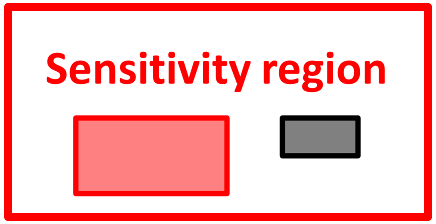

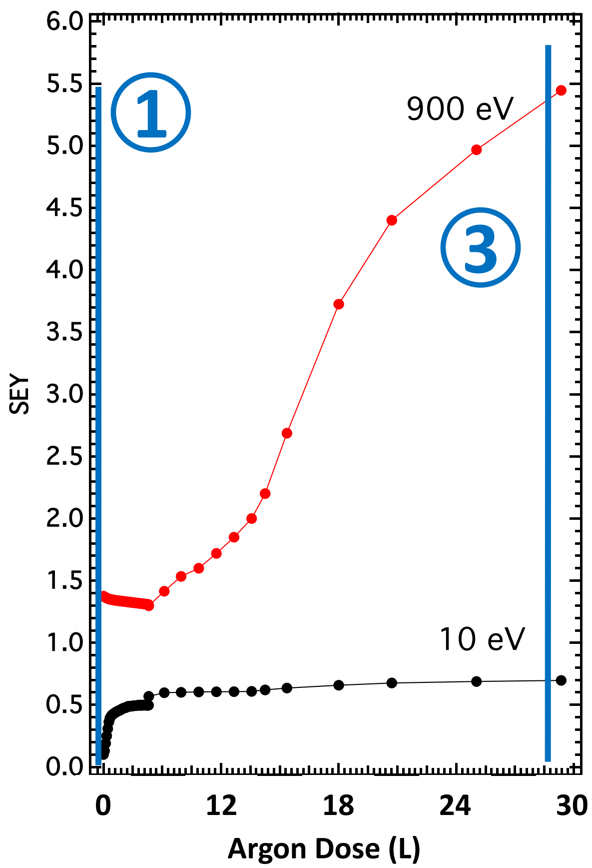

Adsorption monitored by SEY

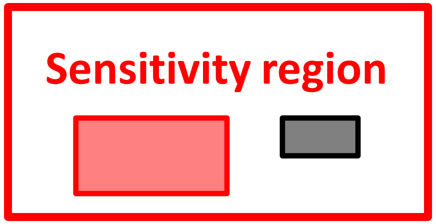

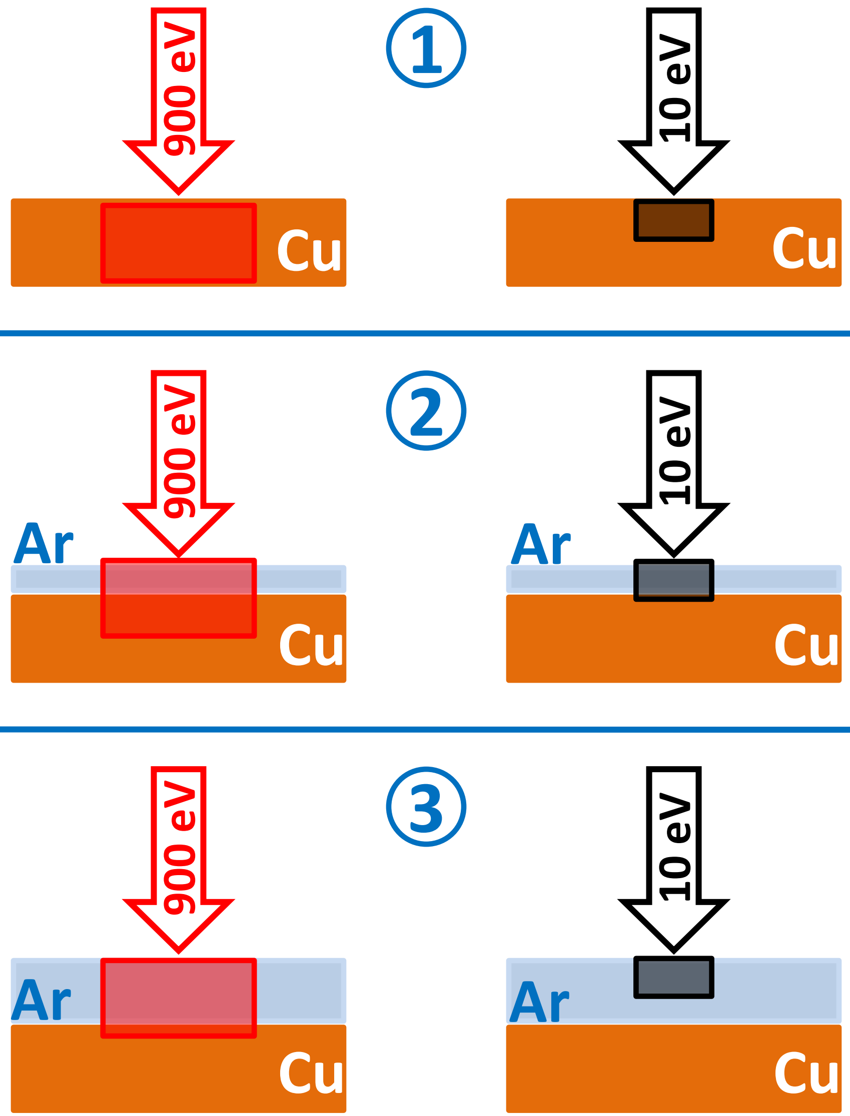

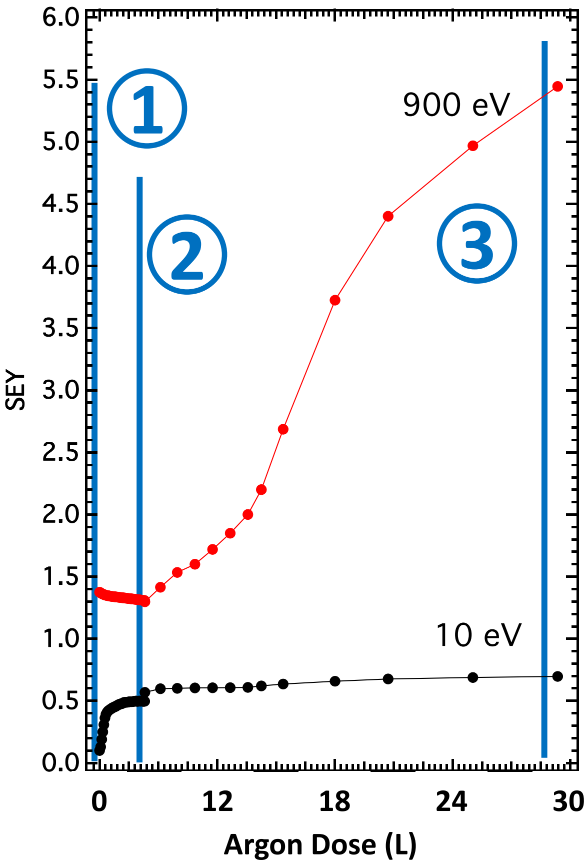

Adsorption monitored by SEY

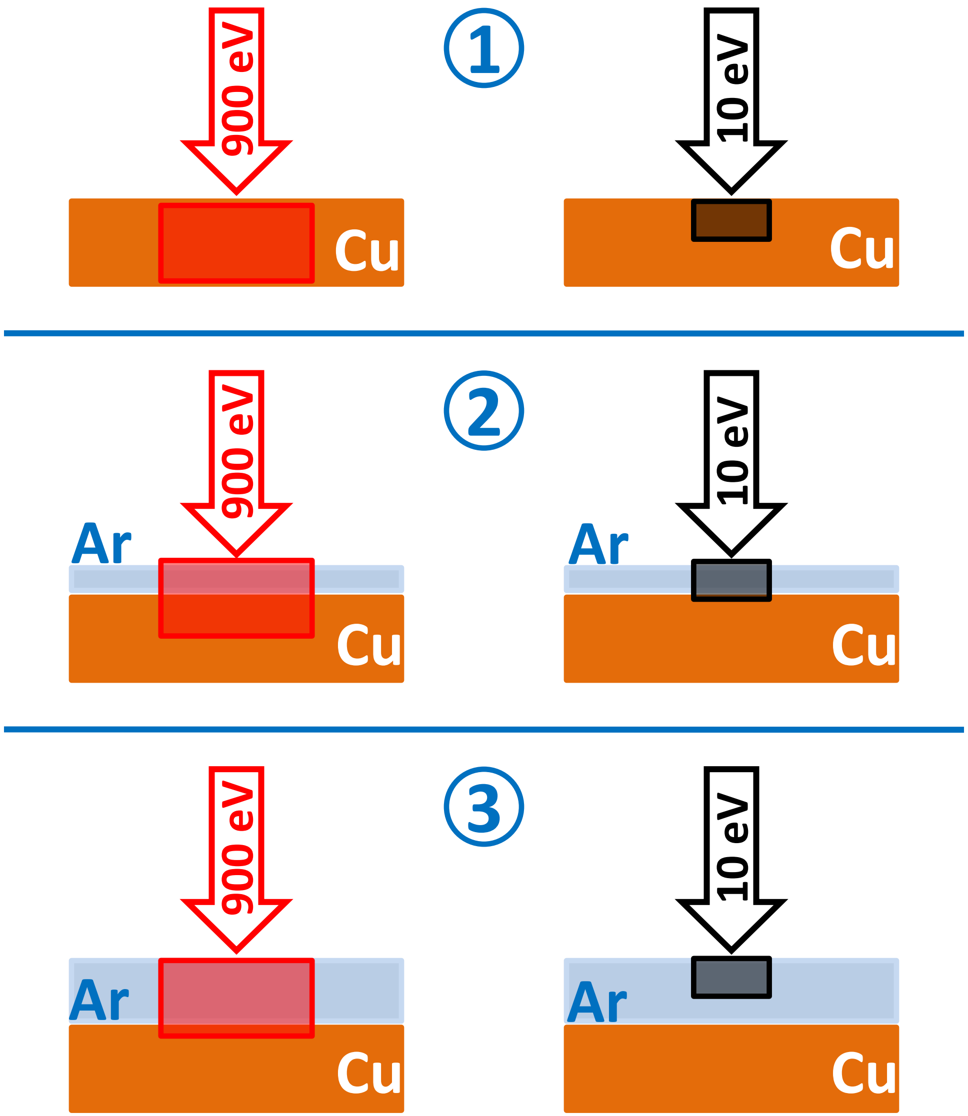

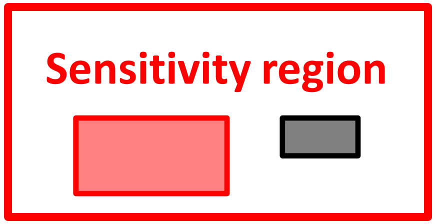

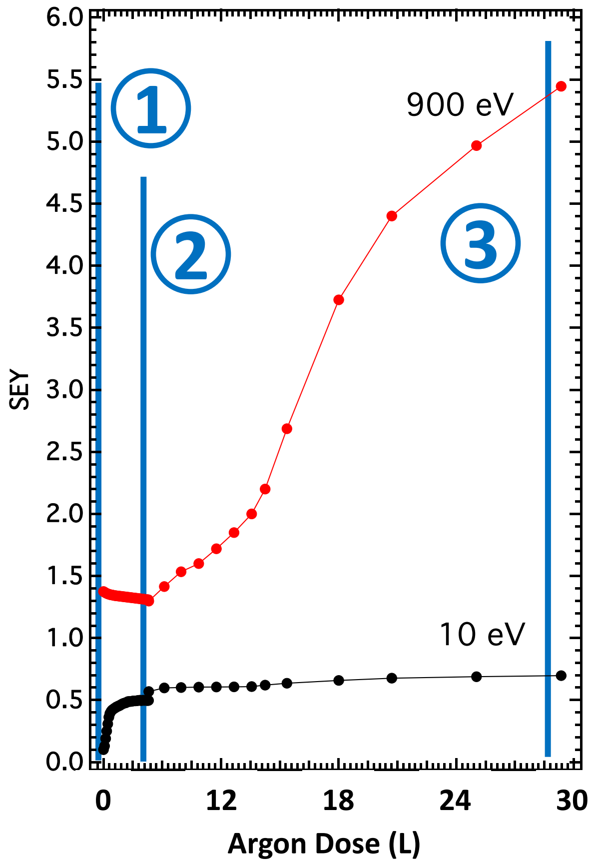

Distinguish single layer from thick film formation by Low-Energy SEY (LE-SEY)

Desorption kinetics by SEY and TPD

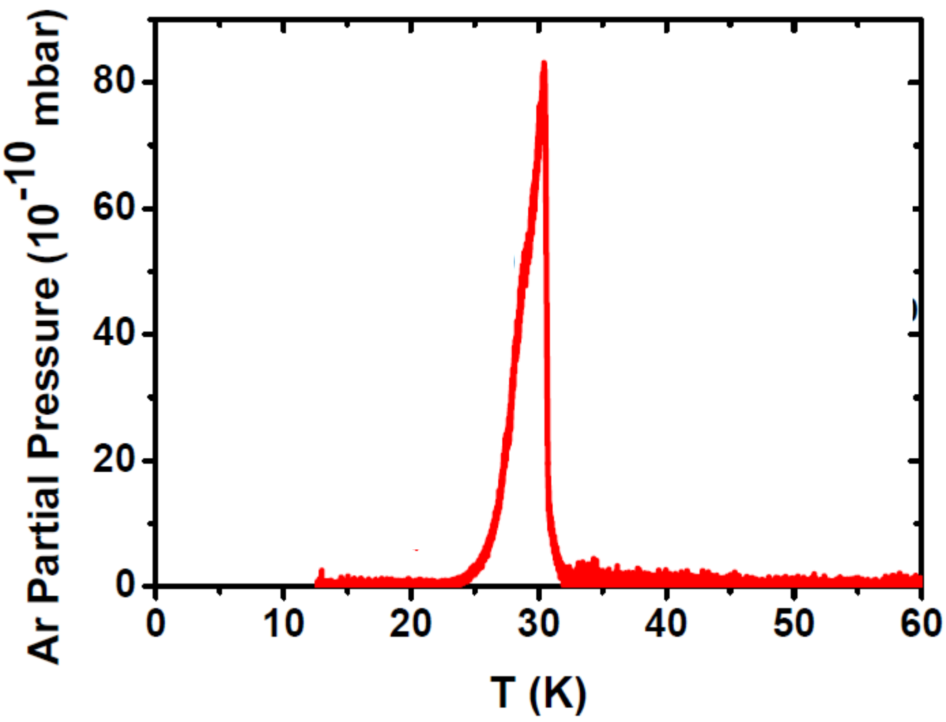

TPD curve obtained in the representative case of 100 L of Ar on a clean Cu substrate

Desorption kinetics by SEY and TPD

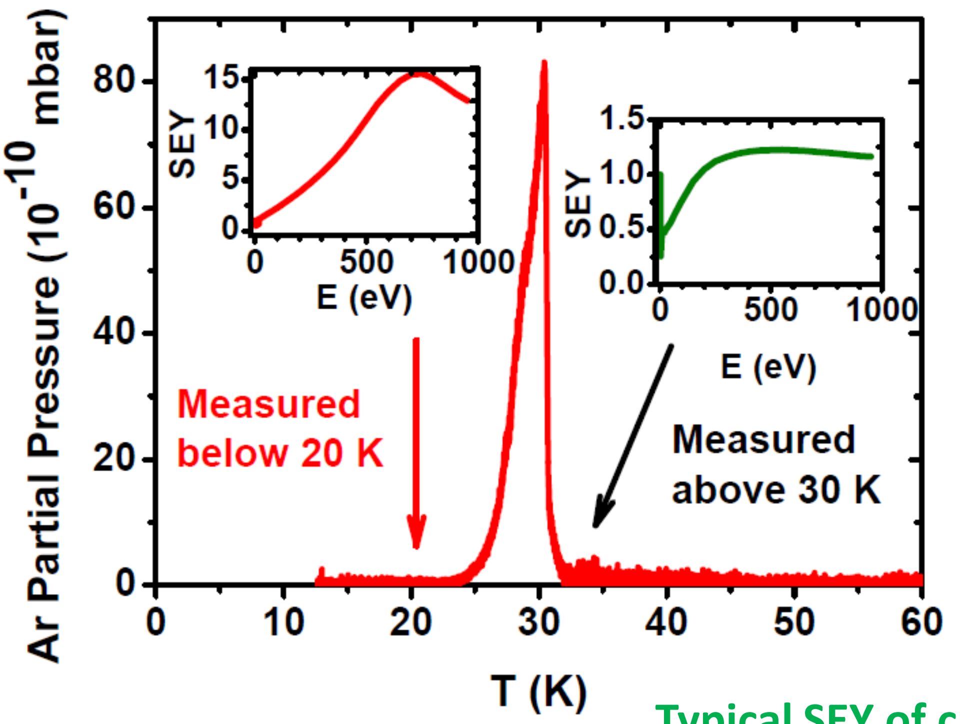

TPD curve obtained in the representative case of 100 L of Ar on a clean Cu substrate

NOTE:

e^- beam current < $1x10^{-7}$ Amp

SEY ideal technique for e^--desorption studies!!!

Typical SEY of clean Cu

(Ar is fully desorbed)

Typical SEY of 100 L Ar on Cu

SEY measurements performed during the thermal desorption process

Measure the desorption temperature with SEY

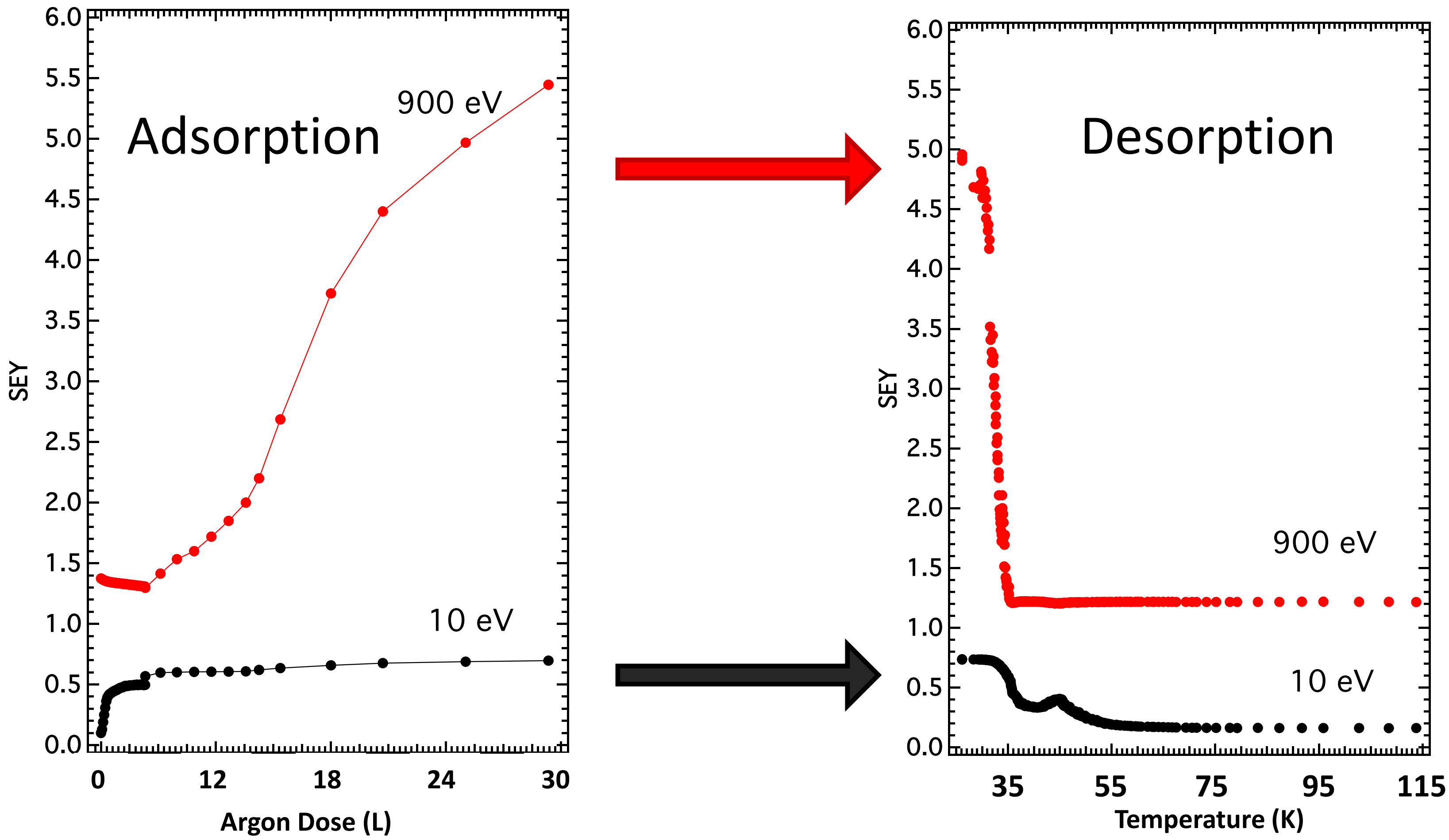

Measure the desorption temperature with SEY

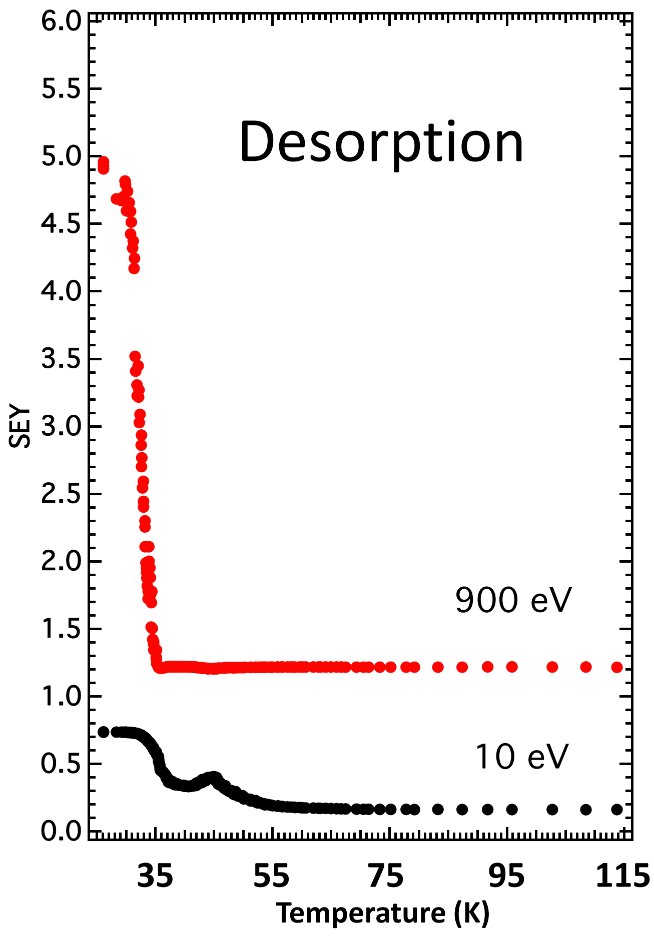

Measure the desorption temperature with SEY

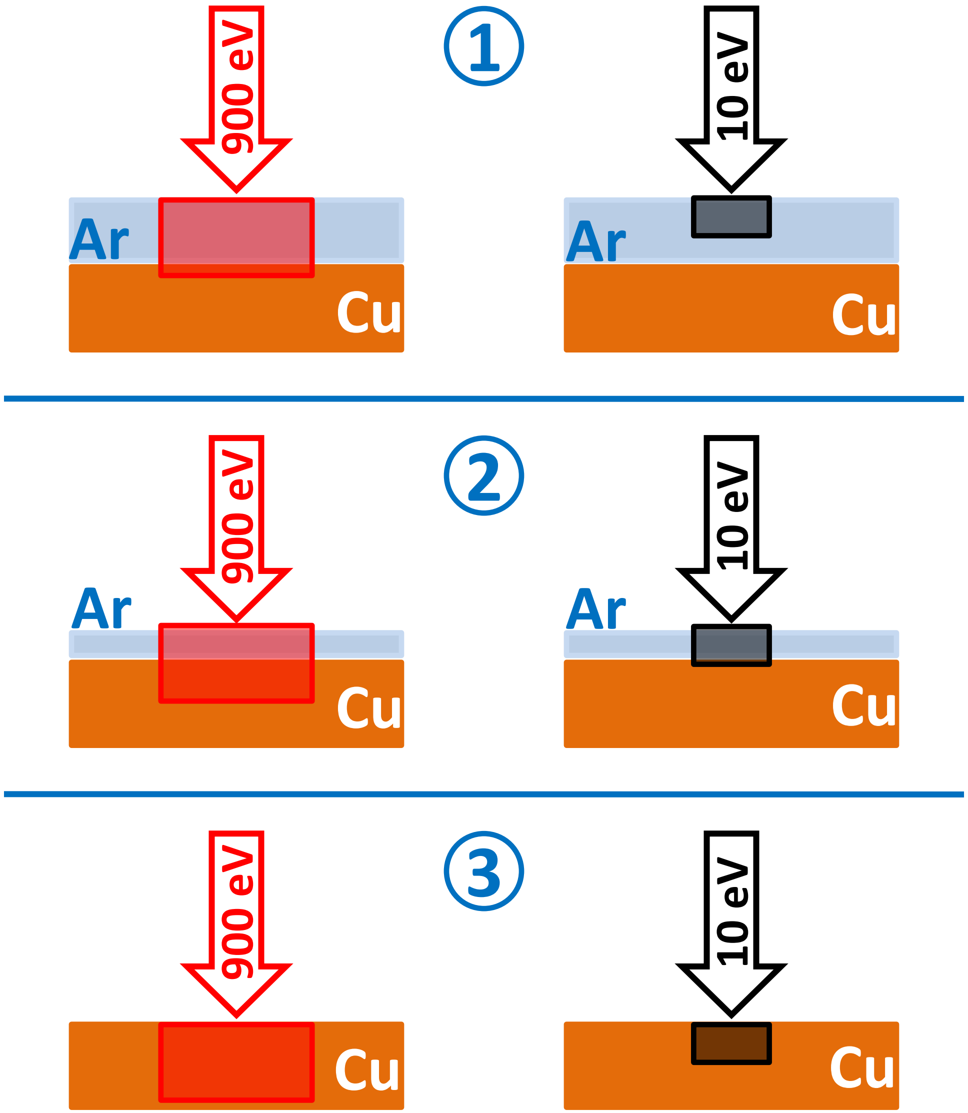

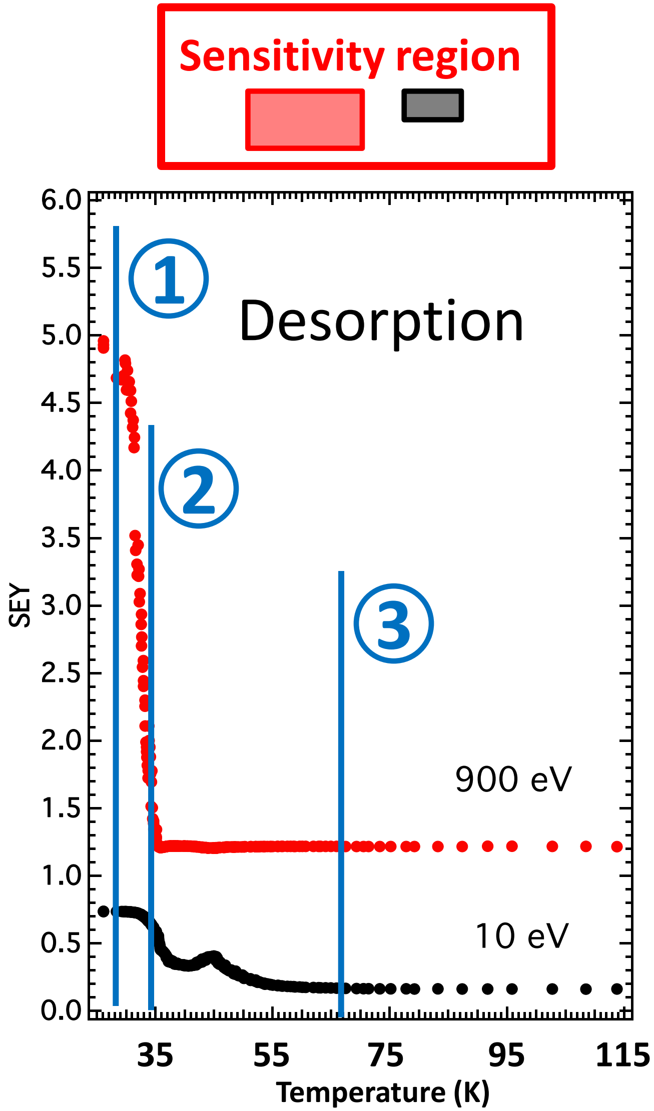

Measure the desorption temperature with SEY

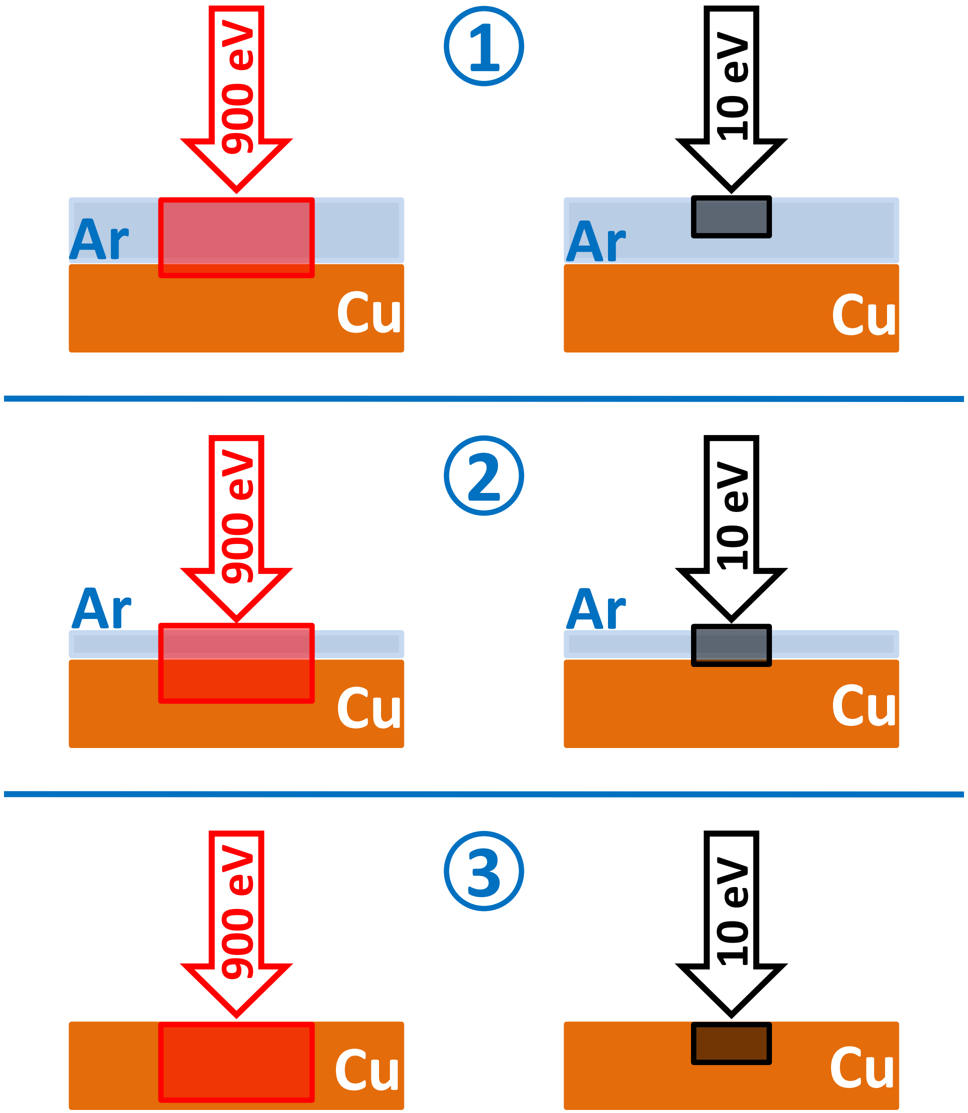

Measure the desorption temperature of thick film and single layer by SEY

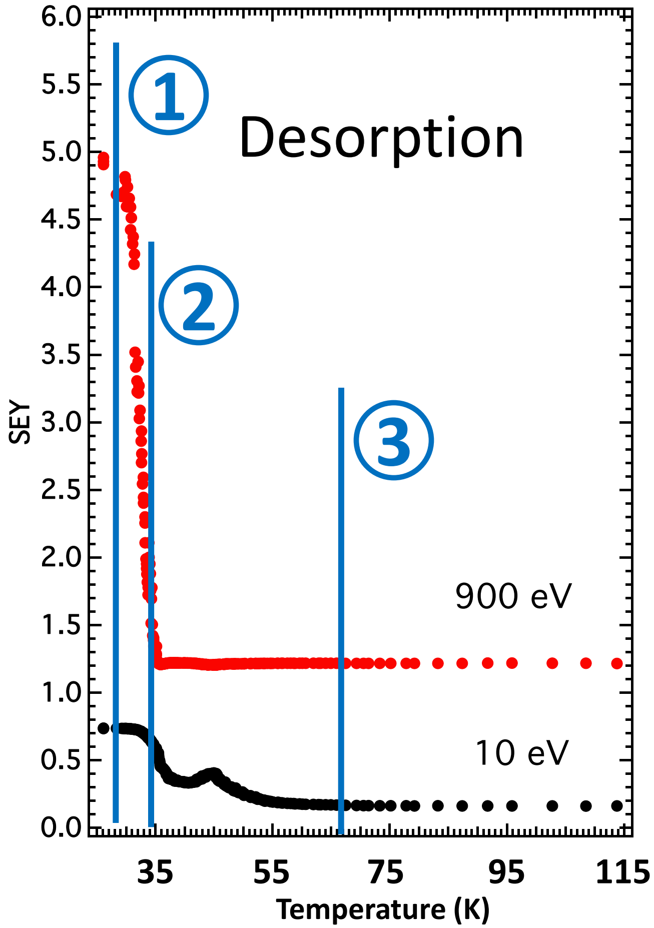

TPD of Ar on LASE-Cu for vacuum stability studies

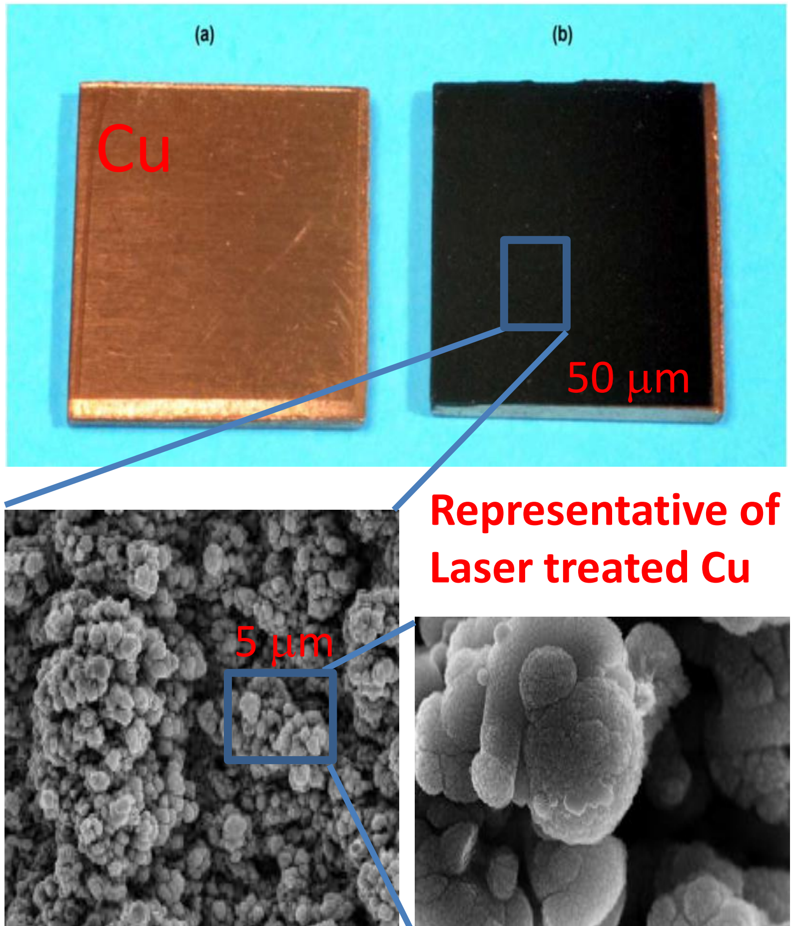

R. Valizadeh et al., Appl. Surf. Sci. (2017)

Ideal δ <1

What about the influence of the surface features on the vacuum stability?

R. Valizadeh et al. , Appl. Phys. Lett. (2014)

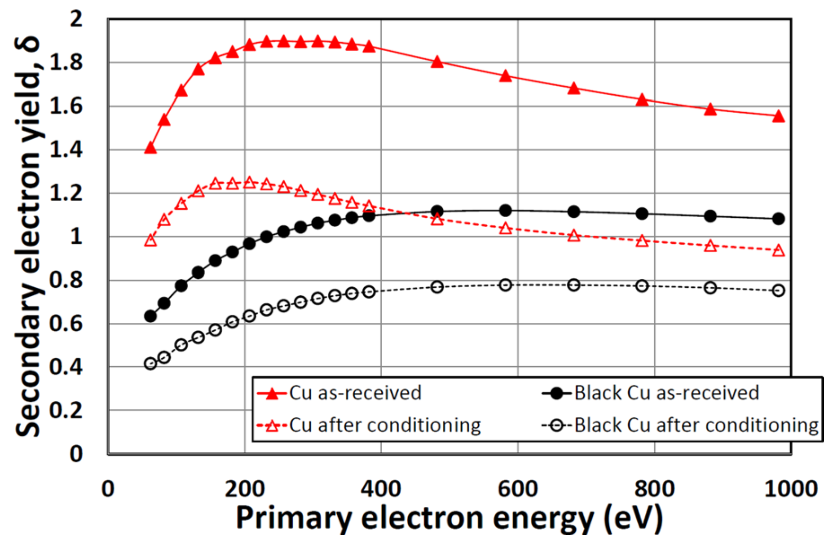

TPD of Ar on LASE-Cu for vacuum stability studies

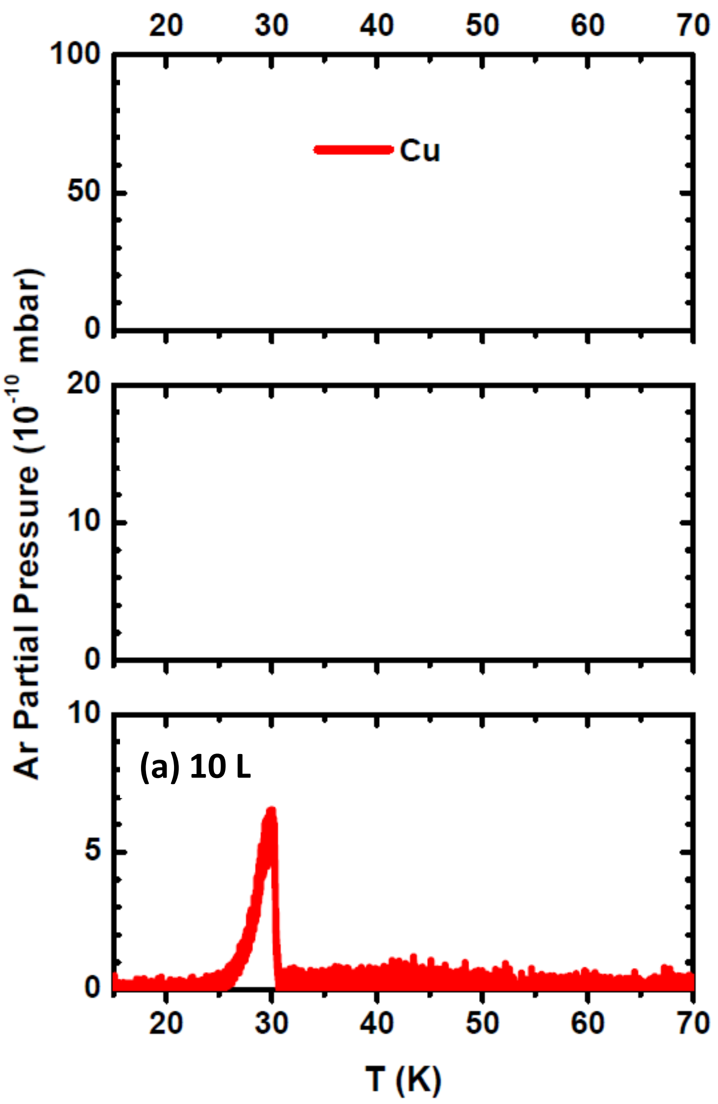

TPD curves obtained from desorption of different doses of Ar on a **clean Cu**

TPD of Ar on LASE-Cu for vacuum stability studies

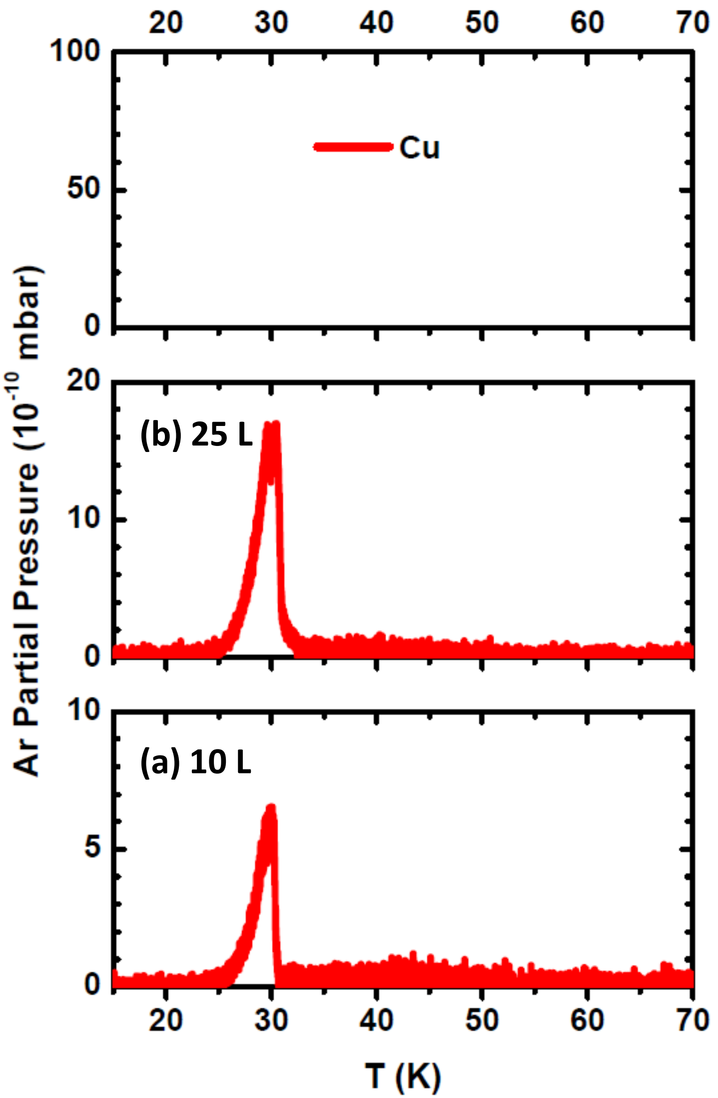

TPD curves obtained from desorption of different doses of Ar on a **clean Cu**

TPD of Ar on LASE-Cu for vacuum stability studies

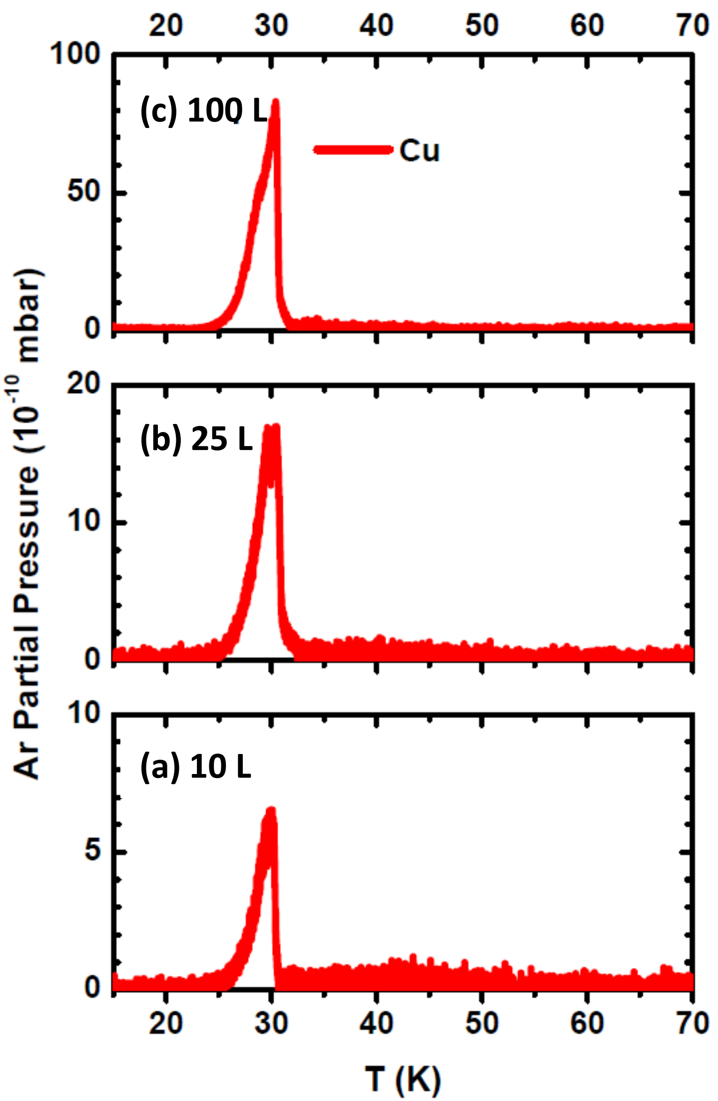

TPD curves obtained from desorption of different doses of Ar on a **clean Cu**

- On **flat Cu** Ar adsorbs due to the weak Ar-Cu and Ar-Ar Van der Waals interactions and the desorption curve consists of the sharp peak at T~30 K.

TPD of Ar on LASE-Cu for vacuum stability studies

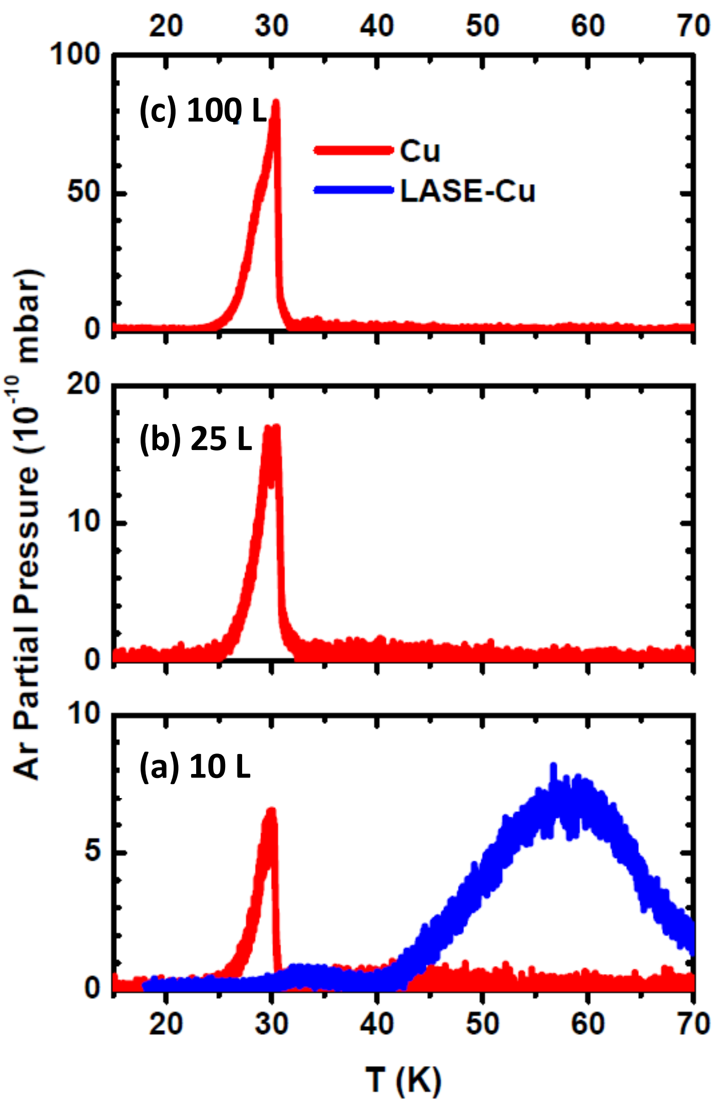

TPD curves obtained from desorption of different doses of Ar on a **clean Cu** and **LASE-Cu** substrate

- On **flat Cu** Ar adsorbs due to the weak Ar-Cu and Ar-Ar Van der Waals interactions and the desorption curve consists of the sharp peak at T~30 K.
- For the **LASE-Cu** substrate the Ar adsorption energy at the under-coordinated surface defect sites increases and desorption occurs at higher T.

TPD of Ar on LASE-Cu for vacuum stability studies

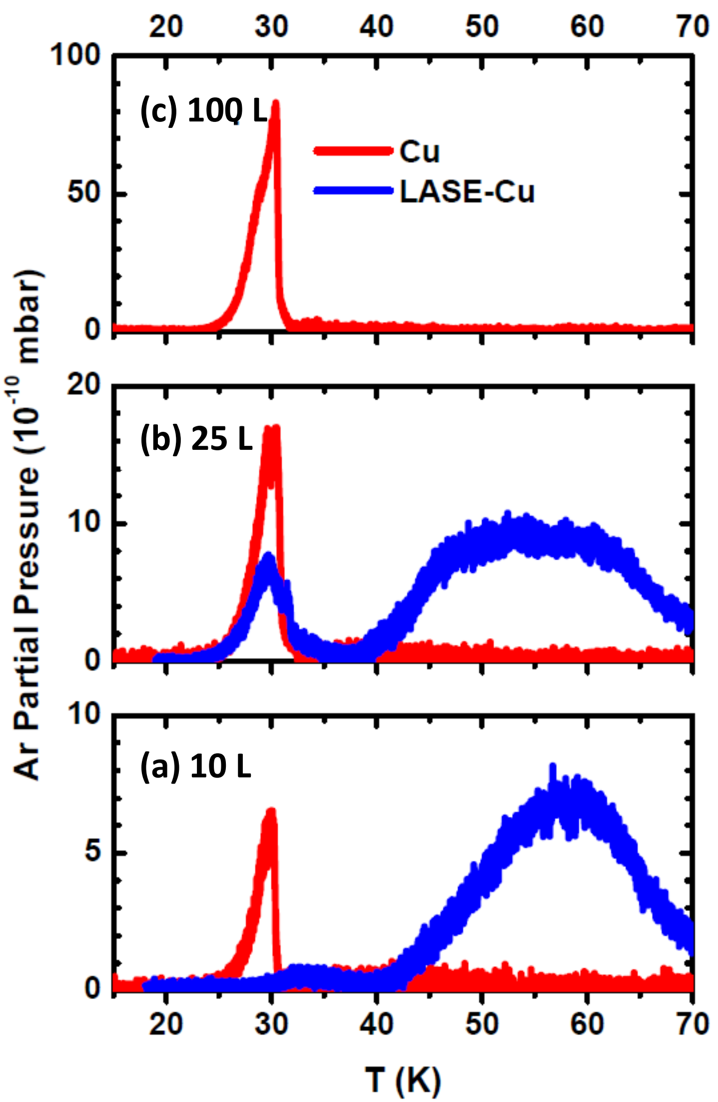

TPD curves obtained from desorption of different doses of Ar on a **clean Cu** and **LASE-Cu** substrate

- On **flat Cu** Ar adsorbs due to the weak Ar-Cu and Ar-Ar Van der Waals interactions and the desorption curve consists of the sharp peak at T~30 K.
- For the **LASE-Cu** substrate the Ar adsorption energy at the under-coordinated surface defect sites increases and desorption occurs at higher T.

TPD of Ar on LASE-Cu for vacuum stability studies

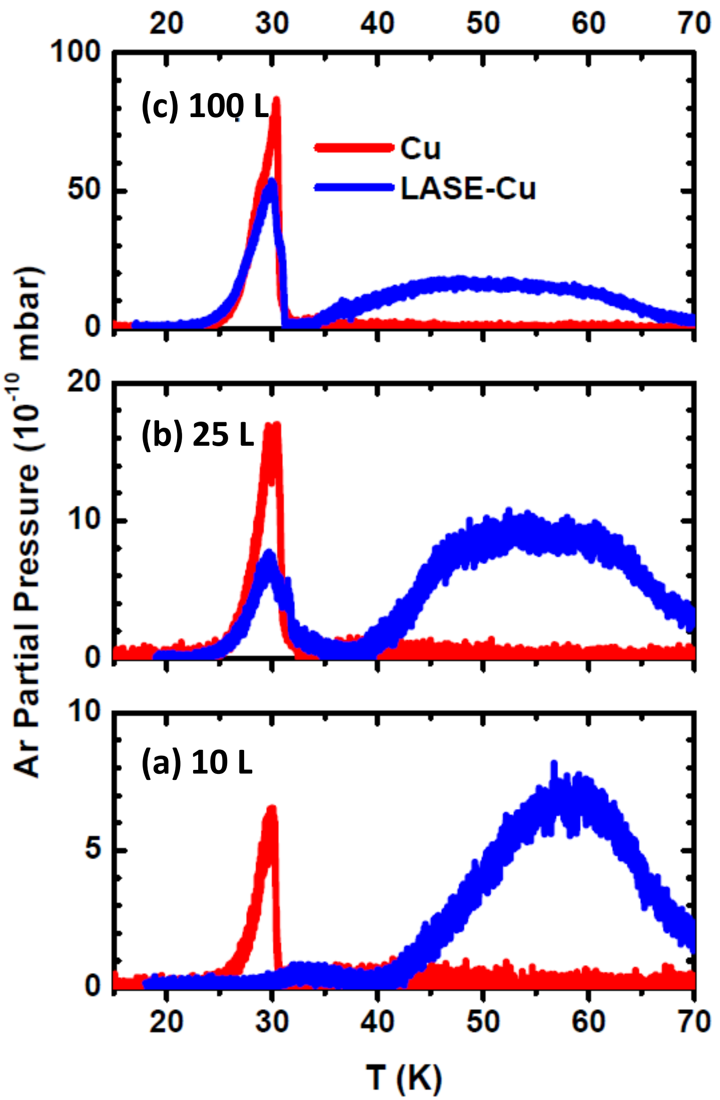

TPD curves obtained from desorption of different doses of Ar on a **clean Cu** and **LASE-Cu** substrate

- On **flat Cu** Ar adsorbs due to the weak Ar-Cu and Ar-Ar Van der Waals interactions and the desorption curve consists of the sharp peak at T~30 K.

- For the **LASE-Cu** substrate the Ar adsorption energy at the under-coordinated surface defect sites increases and desorption occurs at higher T. However, at high coverage, multilayer desorption at T~30 K is also observed.

D. E. Lott, Geochem. Geophy. Geosy. (2001)

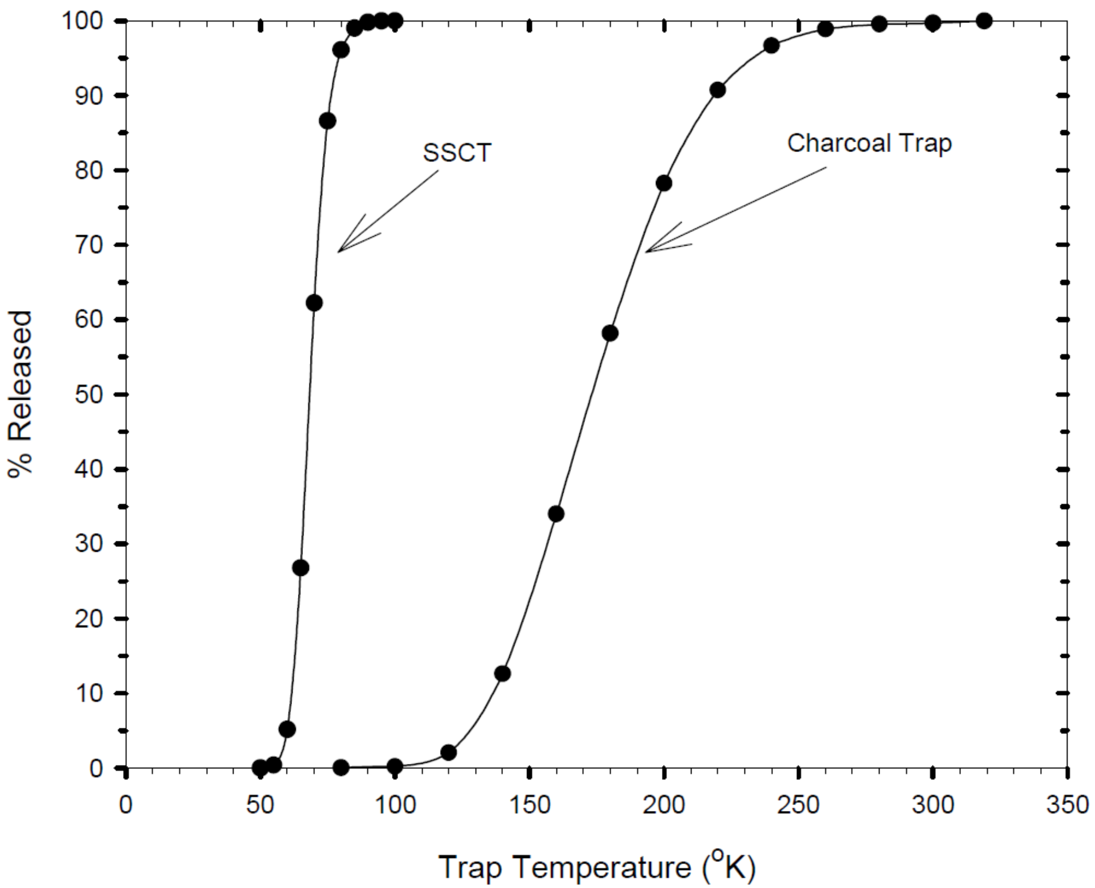

Desorption processes in charcoal and other cryotraps

Comparison of the Stainless Steel CryoTrap (SSCT) and charcoal cryogenic trap release characteristics for argon as a function of temperature

Spread of the desorption temperature range

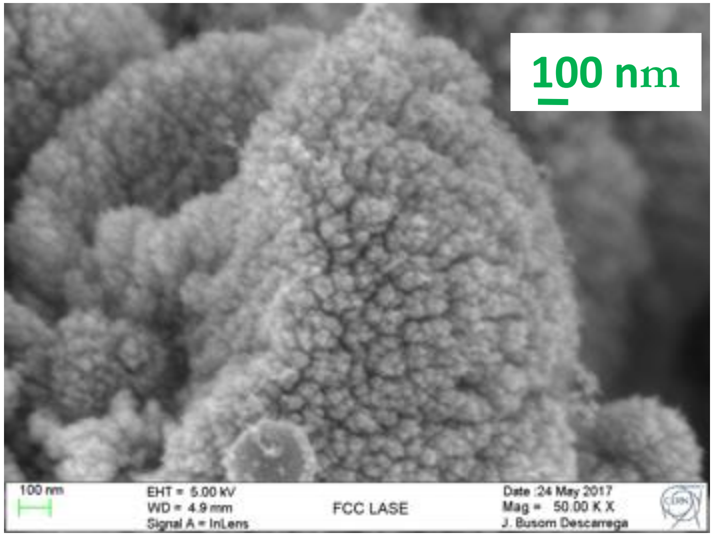

Morphology of LASE-Cu by SEM

Highly rough and inhomogeneous surface with nanometric features (undercoordinated surface defect sites)

At higher coverages the desorption is dominated by usual Ar/Ar Van-der-Waals interaction

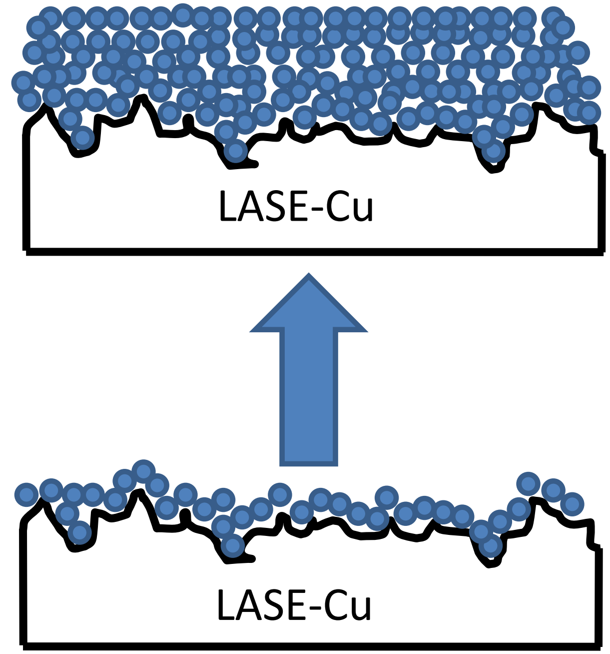

At low coverages the desorption is dominated by Ar/LASE interaction

Implication for the vacuum stability

Saturated vapour pressure from Honig and Hook (1960) (C2H6 Thibault et al.)

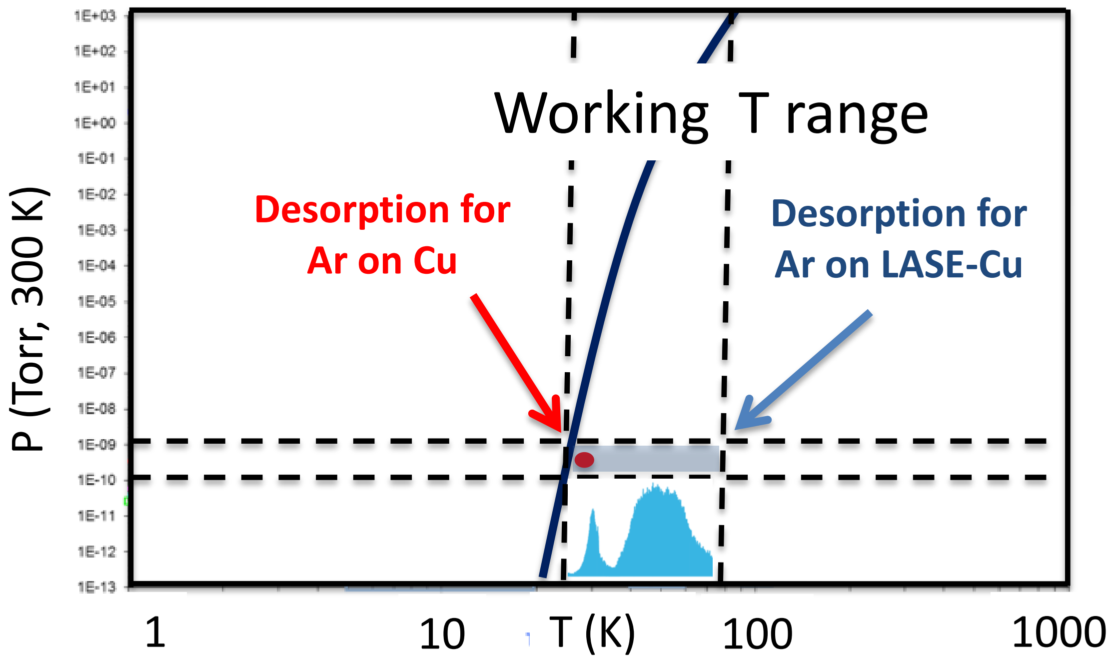

For ices dominated by Ar-LASE, Ar desorbs both at T~ 25-30 K and in a much wider range

Concluding remarks

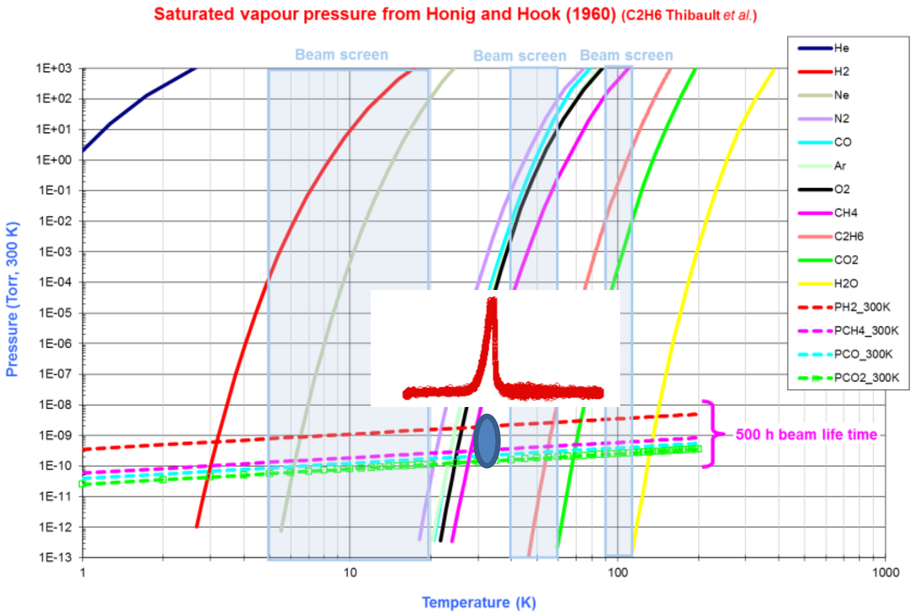

WARNING: **If confirmed also with other molecular species, the use of highly porous materials at cryogenic temperature must be considered with great care!**

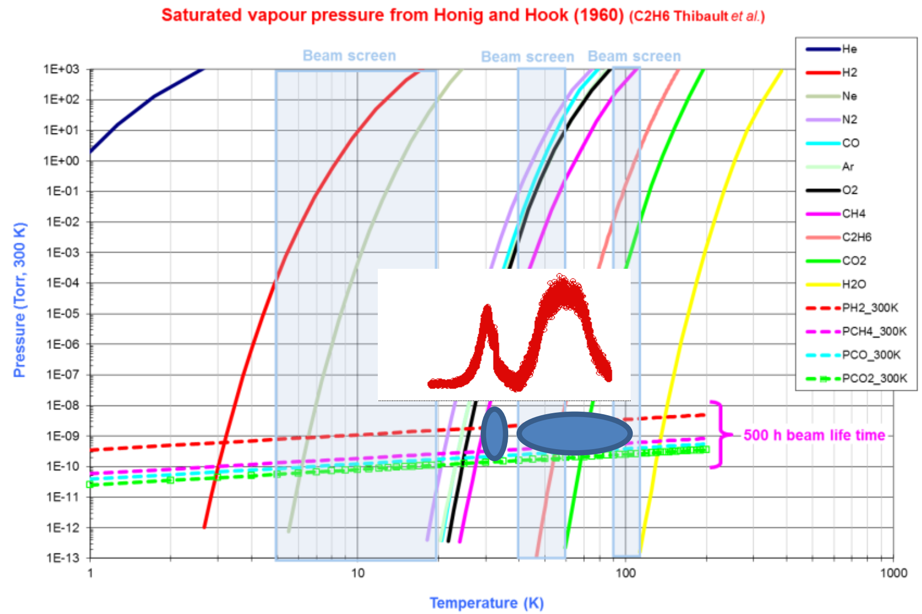

Concluding remarks

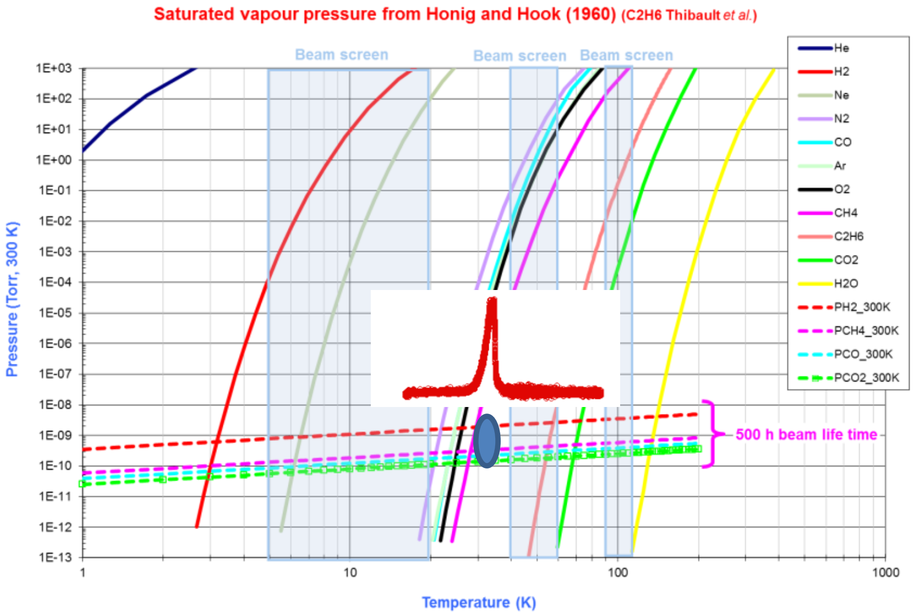

WARNING: If confirmed also with other molecular species, the use of highly porous materials at cryogenic temperature must be considered with great care!

Surface properties of materials, which are useful in the context of particle accelerators, have to be carefully evaluated from all points of view, considering both requirements and constrains.

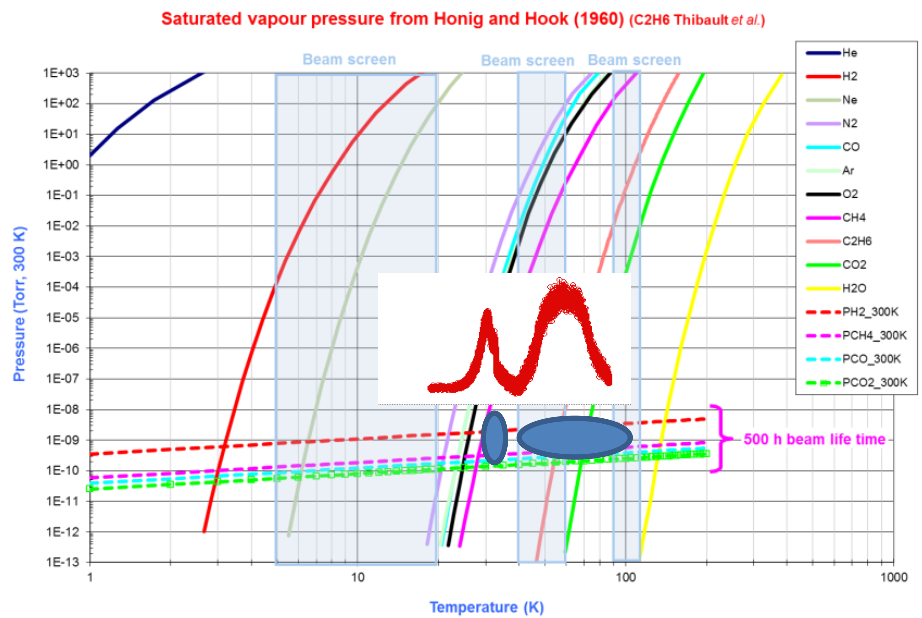

Thank you for your attention

and thanks to….

E. La Francesca R. Cimino R. Larciprete

A. Liedl

M. Angelucci

The team at LNF

EuroCirCol A key to New Physics

INFN LNF Istituto Nazionale di Fisica Nucleare Divisione Ricerca: DAFNEL